

## ORIGINAL ARTICLE

# Prediction of total carotenoids, color, and moisture content of carrot slices during hot air drying using non-invasive hyperspectral imaging technique

Rosalizan Md Saleh<sup>1,2</sup>  | Boris Kulig<sup>1</sup>  | Arman Arefi<sup>1</sup>  | Oliver Hensel<sup>1</sup>  |  
Barbara Sturm<sup>1,3,4</sup> 

<sup>1</sup>Department of Agricultural and Biosystems Engineering, University of Kassel, Witzenhausen, Germany

<sup>2</sup>Industrial Crops Research Centre, Malaysian Agricultural Research and Development Institute (MARDI), Serdang, Selangor, Malaysia

<sup>3</sup>Leibniz Institute for Agricultural Engineering and Bioeconomy (ATB), Potsdam, Germany

<sup>4</sup>Albrecht Daniel Thaer - Institute of Agricultural and Horticultural Sciences, Humboldt Universität zu Berlin, Berlin, Germany

## Correspondence

Rosalizan Md Saleh, Department of Agricultural and Biosystems Engineering, University of Kassel, Witzenhausen, Germany.

Email: [rosalizansaleh@gmail.com](mailto:rosalizansaleh@gmail.com)

## Funding information

Bundesanstalt für Landwirtschaft und Ernährung, Grant/Award Number: BLE - 2817OE005; German Research Foundation (DFG-Deutsche Forschungsgemeinschaft), Grant/Award Number: Project number: 420778578; Institut Penyelidikan dan Kemajuan Pertanian Malaysia; Federal Ministry of Food and Agriculture; Coordination of European Transnational Research in Organic Food and Farming Systems; the Universität Kassel

## Abstract

The objective of this paper was to evaluate the performance of Partial Least Square Regression (PLSR) model and to assess the statistical agreement between two different measurement techniques, that is, Vis-NIR hyperspectral imaging (HSI) and standard laboratory methods for quality evaluation of dried carrots throughout the hot-air drying process. Carrots at commercial maturity of 3.5 months after planting were harvested in two seasons (2017 and 2018) and dried in a convective hot air dryer at 50°C, 60°C, and 70°C. Quality measurements were examined at intervals of 30 minutes. PLSR was performed as a regression model to predict quality attributes in carrots, while Passing-Bablok and Deming regressions alongside Blant-Altman analysis were applied as method comparisons. Excellent prediction performance for moisture content was observed with high  $R^2_T$  and  $R^2_V$  at 0.92 and 0.90 with values of  $RMSE_T$  and  $RMSE_V$  at 8.15% and 8.16%. Satisfactory prediction accuracies were observed for total carotenoids ( $R^2_V = 0.64$  and  $RMSE_V = 32.62$ )  $\mu\text{g/g}$ ,  $L^*$  ( $R^2_V = 0.68$  and  $RMSE_V = 32.62$ ),  $a^*$  ( $R^2_V = 0.69$  and  $RMSE_V = 1.18$ ), and  $b^*$  ( $R^2_V = 0.60$  and  $RMSE_V = 1.45$ ). Selected wavelengths for total carotenoids, moisture content,  $L^*$ ,  $a^*$ , and  $b^*$  based on the highest score of VIP loadings were 531, 973, 531, 531, and 680 nm, respectively. An adequate agreement of Blant-Altman analysis between the two methods within the upper and lower limits of 95% confidence interval (CI) were obtained for total carotenoids from 95.68  $\mu\text{g/g}$  to 82.34  $\mu\text{g/g}$ , moisture content (25.18% to 22.93%),  $L^*$  (2.88 to -3.30),  $a^*$  (4.15 to 3.43), and  $b^*$  (4.53 to -3.11) with mean differences at 6.67, 1.12, -0.21, 0.36, and 0.71, respectively. Good correlation coefficients ( $r$ ) were also observed at 0.89, 0.91, 0.78, and 0.83 for moisture content,  $L^*$ ,  $a^*$ , and  $b^*$  with a moderate correlation of total carotenoids at 0.69. The results indicate the potential feasibility of using non-invasive measurement of quality attributes using hyperspectral imaging during the drying of carrots.

## Novelty impact statement

- non-invasive measurement using hyperspectral imaging for quality determination in carrots during convective drying demonstrated promising results.

This is an open access article under the terms of the [Creative Commons Attribution](https://creativecommons.org/licenses/by/4.0/) License, which permits use, distribution and reproduction in any medium, provided the original work is properly cited.

© 2022 The Authors. *Journal of Food Processing and Preservation* published by Wiley Periodicals LLC.

- Multivariate analysis of Partial Least Square Regression showed a good modeling performance for quality prediction in dried carrots.
- A good statistical agreements between non-invasive quality measurements using hyperspectral imaging and standard laboratory analysis were achieved by comparative analysis using Blant–Altman plot, Deming, and Passing–Bablok regression.

## 1 | INTRODUCTION

Fruits and vegetables provide essential nutrients and minerals with significant health benefits to humans. Adequate intake of fruits and vegetables for daily consumption is recommended for health maintenance and disease prevention (Slavin & Llyod, 2012). One of the most popular and nutritious vegetable crops with an appreciable amount of phytochemical constituents is the carrot (Ahmad et al., 2019). Carrots are considered as a primary vegetable in many countries and the crop is widely cultivated and consumed globally due to its nutraceutical properties and culinary attributes with pleasant taste and flavors (Surbhi et al., 2018; Liu et al., 2016; Arscott & Tanumihardjo, 2010). The roots are rich in phytonutrients such as carotenoids (particularly  $\beta$ -carotenes), phenolic compounds, dietary fibers, and minerals. All these bioactive components possess specific health-promoting properties with a great potential for providing a protection mechanism against coronary heart disease and certain cancers (Surbhi et al., 2018; Da Silva Dias, 2014). Carrots can be eaten fresh and cooked into a variety of dishes or it can be processed into puree, juices, or dehydrated products (Nguyen & Nguyen, 2015; Arscott & Tanumihardjo, 2010). Fresh carrots can be converted into dehydrated form by drying and the dried carrots can be commercially used as a natural ingredient for the formulation and development of functional products such as dietary supplements, nutraceuticals, and cosmetics (Nguyen & Nguyen, 2015; Igielska-Kalwat et al., 2012; Anunciato & da Rocha Filho, 2012). The demand for dried carrots also rises in the instant food industry since the dried roots can be mixed with other ingredients for the development of instant soups and meals (Koca et al., 2007).

To this end, food producers are competing to produce high-quality of dried products with the need to have a reliable, accurate, and rapid assessment device for efficient quality assurance that could be advantageous for the food industry with an objective to minimize the overall operational time as well as to meet the consumer's demand. Monitoring product quality along the production chain is very important in food processing in order to ensure the safety and quality of the end product (Pu et al., 2015).

In recent years, various non-destructive methods have been researched extensively and tested to evaluate the quality of fruits and vegetables starting from farm to retail market and some of them have commercially been applied for food grading and sorting in the packing houses and food processing lines (Kamal et al., 2019; Nicolai et al., 2014). One of the most recent investigated non-destructive techniques is a hyperspectral imaging (HSI) which is capable to generate both spectral information and a spatial map simultaneously at a certain

range of wavelengths and the acquired spectra are qualitatively related to the physical and chemical properties of the product. The key principle of HSI is by integrating both imaging technology coupled with spectrophotometry and this new hybrid technology has been comprehensively studied for evaluating the physical properties and internal qualities of fruits and vegetables during drying (Arefi et al., 2021; von Gersdoff et al., 2021; Sturm et al., 2020; Yu et al., 2020; Amjad et al., 2019; Liu et al., 2017). Recently, the potential usage of hyperspectral imaging was also documented for the identification of saccharin jujube (Zhang et al., 2020) and the retention of anthocyanin in purple-fleshed sweet potato during convective and microwave drying (Tian et al., 2021).

The applicability of this new generation of sensing technology for non-invasive measurement techniques has intensively been studied over the past 10 years in order to develop a quick, simple, chemical-free procedure and convenient application for quality evaluation of food materials during processing (Zhang et al., 2018). The use of existing standard laboratory analyses can be time-consuming, labor intensive, and require expert and skillful laboratory personnel with complex sample preparations and hazardous solvents. Moreover, the utilization of expensive instruments could contribute to the additional operating and maintenance cost. Therefore, it is necessary to explore and establish a new technology for rapid and effective quantification methods that could potentially be applied for online and real-time quality assessment during drying since this technique enables an automatic prediction of the quality attributes of fruits and vegetables in a non-destructive manner.

The most notable benefit of HSI is the ability to identify various components simultaneously and this method provides scientific tools for non-destructive quality inspection with minimal sample preparation and rapid acquisition times with simultaneous visualization of the spatial distribution of numerous chemical components (Elmasry & Sun, 2010; Wu & Sun, 2013). The spectral data include two-dimensional spatial vector array reflecting the spectrum at each pixel of the 3D image with a three-dimensional data set which is known as the data cube or hypercube. The resulting spectra from HSI must be extracted, processed, and interpret by means of chemometric methods, so that the large data set can be transformed into useful information, and finally a relationship between the target attributes and their corresponding hyperspectral data of the tested samples can be established (Bro et al., 2002). The most common chemometric algorithms are regression algorithms which can be classified into linear and nonlinear analysis such as partial least square regression (PLSR) (Pan et al., 2016). PLSR technique is widely used in the modeling of hyperspectral data due to its versatility in multivariate approaches and this model was performed for data computation in this study.

The ability of HSI to generate a large amount of spectral data over a wide range of wavelengths causes sizable amounts of redundant information due to multicollinearity with high covariance which requires high storage capacity and lengthy processing time (Baek et al., 2019; He & Sun, 2015). Therefore, the optimal variable selection method based on the Variable Importance in Projection (VIP) scores needs to be carried out in order to extract the most influential wavelengths in the multivariate models for specific quality attributes. The main goal of selecting the feature wavelengths is to improve the validation performance while eliminating uninformative data and thus, reducing the computation time (Baek et al., 2019; Chen et al., 2014). A higher VIP score indicates greater importance of the respond variable as a predictor (Rahman et al., 2018). Normally, a threshold value of VIP scores between 0.83 and 1.21 is highly significant and recommended (Chong & Jun, 2005).

For many years, regression analysis which is in accordance with the correlation coefficient has been used to evaluate and describe the strength of a relationship between two variables without providing their agreement (Doğan, 2018; Bilic-Zulle, 2011). The range of the correlation coefficient ( $r$ ) from  $-1.0$  to  $+1.0$  indicates the strength level of the linear relationship between variables. The higher the correlation coefficient, the greater the strength of the relationship. However, according to Doğan (2018), a strong correlation does not necessarily suggest that the two methods can be performed interchangeably with a good agreement. In addition, data that appear to be in a weak agreement may generate very strong correlations or vice versa (Doğan, 2018). The comparative methods are necessary to confirm the reliability, stability, and accuracy of the new method whether it can be used interchangeably and replacing the conventional laboratory method for estimating the quality parameters of carrots during drying. This statistical approach is very common in medical science and clinical research, but very limited studies have been published on its application in the food science. This approach is very useful if a new measurement technique which has some advantages needs to be introduced over an existing measurement method (Gold standard). The new potential method must be validated in order to demonstrate its equal reliability, precision, and repeatability for the intended usage. The most common statistical analysis for method comparisons is Passing–Bablok and Deming regressions (Haeckel et al., 2013) as well as Blant–Altman analysis (Hanneman, 2008).

The Blant–Altman plot shows the mean difference between the measurements by two methods (vertical axis) and their mean (horizontal axis) with the addition of agreement limits (Hofman et al., 2015). Blant–Altman plots are commonly used to evaluate the agreement between two different instruments or two techniques of measurement such as comparing a new technique of non-destructive quality measurement using HSI with a gold standard of laboratory analysis in this study. Blant–Altman plots also allow any systematic discrepancy between measurements (i.e., fixed bias) or potential outliers to be possibly detected (Hannemen, 2008), while Passing–Bablok assumes both methods are highly correlated having a linear relationship (Passing and Bablok, 1983). Deming regression can be

helpful and favorable for comparing analytical methods due to its robustness against outliers. This method also considers measurement errors between the test and reference methods (Giavarina, 2015; Cornbleet & Gochman, 1979).

In light of this, a new approach of method comparison using both regression techniques of Passing–Bablok and Deming regressions combined with Blant–Altman analysis will be tested in this study for assessing and comparing the performance of this new method of non-destructive measurement using HSI with a standard laboratory method.

The main objectives of the current study were as follows: (1) To evaluate the performance of PLSR modeling for predicting the quality attributes in carrots during drying, (2) To determine the important wavelengths which correspond to specific quality attributes based on the highest score of Variable Importance in Projection plots (VIP), and (3) To evaluate the statistical agreement between conventional laboratory methods with non-destructive measurements of HSI using Passing–Bablok and Deming regressions alongside with Blant–Altman analysis for method comparisons.

## 2 | MATERIAL AND METHODS

### 2.1 | Raw materials

Organic carrots (*var. Laguna*) at an optimum maturity of 3.5 months after planting were harvested at different seasons during autumn (2017) and summer (2018) from the University of Kassel's farm in Frankenhausen, Kassel, Germany. All carrots from both seasons were harvested in the morning prior to drying experiments. The average daily temperatures for both seasons were  $16^{\circ}\text{C}$  and  $28^{\circ}\text{C}$ , respectively. Therefore, the harvested roots were observed to have different characteristics with large variations of total carotenoids content and color intensity. The observations were confirmed by a study conducted by Brunsgaard et al. (1994). The authors reported significant variations of chemical compositions in different varieties of carrots harvested from two consequent years of 1990 and 1991. After that, the roots were washed with distilled water, peeled, and sliced by using a food slicer (Graef, E21EU, Germany) prior to all drying experiments. The exterior diameter for each slice was kept constant at  $2.5 \pm 0.1$  cm by using a custom-made rounded stainless steel cutter. The diameter of carrots was measured manually using a Vernier caliper (Kinzo, 98,618, Netherlands).

### 2.2 | Drying procedure

Drying experiments from both years were carried out using a small-scale commercial dryer (Innotech Ingenieursgesellschaft, HT mini, Germany) at a constant air rate of  $0.6$  m/s. The dimensions of the dryer are  $50 \times 40 \times 60$  cm ( $L \times W \times H$ ) as in Figure 1. The humidity in the dryer was in the range between 6% and 10%. The first drying experiment which was conducted in 2017 investigated the effect of different drying temperatures and thickness on quality changes in

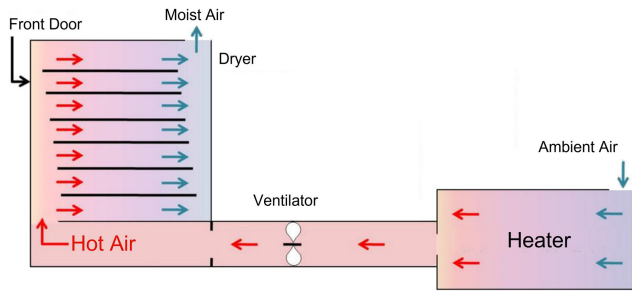


FIGURE 1 Schematic diagram of the dryer

carrots (Md Saleh et al., 2019). In this experiment, about 200 g of sliced carrots of different thicknesses of 3 and 6 mm were placed as a single layer in the dryer and dried at 50°C, 60°C, and 70°C. The second experiment on critical control point-based intermittent drying was carried out in 2018 (Md Saleh et al., 2020). During the trial, 50 g of sliced carrots of the thickness of 3.5 mm was used in the study. The sliced carrots were subjected to different combinations of drying strategies based on intermittency at the critical point of quality degradations. The samples were dried at 60°C and 70°C, and tempering was conducted for 1 and 3 h at 30% and 40% moisture levels. All experiments from both drying strategies were performed in three replicates. Before each drying run, the dryer was started 1 h in advance to reach steady-state conditions. The initial moisture content of carrots was determined according to the AOAC method (2012) by drying the sample in an oven at 105°C for 24 h (Mermert, ULM 400, Germany). The initial moisture content of the fresh carrots was recorded to be around 88% ( $7.54 \text{ g}_w/\text{g}_{dm} \pm 0.3$ ). The drying process for both experiments takes place in a single layer. Samples withdrawal prior to hyperspectral imaging and laboratory analysis for moisture content, color, and total carotenoids throughout the drying period were carried out every 30 minutes for both experiments. For every drying point, four slices from four roots for each replicate were evaluated and a total of 12 slices per drying point were used in this study. The same slices were used for both non-destructive analysis of hyperspectral imaging and laboratory analysis in order to ensure consistency. Moisture content was determined by weighing the samples manually using an electronic balance (Sartorius, E2000D, Germany) until the samples reached a final moisture content of 10% ( $0.10 \pm 0.02 \text{ g}_w/\text{g}_{dm}$ ) (Zhao et al., 2014).

### 2.3 | Measurement of color

Color measurements were performed using a Minolta chroma meter (Minolta, CR-400, Japan). The chroma meter was calibrated against a standard white reference tile prior to sample measurements. The observer used was 2° closely matches CIE 1931 Standard Observer with a silicon photocells detector and a setting illuminant at °C and D65 (Anon, 2002). The color was determined on four slices from four roots at each measurement point for each replicate. For each slice, measurements were taken at two points on the surface and the results were

averaged over the slice. The color measurements were carried out based on the three-dimensional color space of CIE  $L^*a^*b^*$  scale where  $L^*$  represents the brightness of the color,  $a^*$  shows the hue color from red (+) to green (-), and  $b^*$  lies between yellow (+) and blue (-) (Joshi et al., 2009).

### 2.4 | Determination of total carotenoids

Total carotenoids were determined by extracting 100 mg of carrot tissue in a mixture of 10 ml solvent of hexane, acetone, and ethanol at a ratio of 2:1:1 by adopting the method reported by Moscetti et al. (2017). The solution mixture was homogenized for 2 minutes at 8000 rpm by using a laboratory homogenizer (IKA, T25, Germany), and incubated for 1 h at 4°C inside a refrigerator until the sample turned completely colorless in order to ensure all total carotenoids were fully extracted. Then, 5 ml of distilled water was added to the extracted sample to allow phase separation. The upper layer was separated from the aqueous phase and the concentration of total carotenoids was measured at the wavelength of 450 nm by a UV-Vis spectrophotometer (Thermo Electron, Genesys™ 10, USA). The total carotenoids content was finally calculated using Equation (1).

$$\text{Total carotenoids (ml}^{-1}\text{)} = \frac{\text{Abs} * V_1}{A_{1\%}} \times C^{1\%} \quad (1)$$

where Abs is the absorbance reading of the sample,  $V_1$  is the dilution factor,  $A_{1\%}$  is the extinction coefficient of the 1% solution (i.e., 2500 AU) and  $C^{1\%}$  is the concentration of the 1% solution (10 mg/ml). The total carotenoids content was converted to  $\text{mg}/\text{g}_{dm}$  based on dry matter content.

### 2.5 | Hyperspectral imaging system

The image of the samples was captured by employing a hyperspectral imaging system (model: V10E PFD, Specim Spectral Imaging Ltd., Finland) equipped with a 35 mm lens (Schneider Optische Werke GmbH, Xenoplan 1.9/35, Germany) and a linear translation stage (Specim Spectral Imaging Ltd., Finland). The illumination system consisted of three 60 W halogen lamps positioned at an angle of 45°. A set of four slices of carrots along with a white tile were captured at each drying point in the spectral range of 400–1010 nm. A total of 1368 carrot slices from two growing seasons were used in this study. The average spectrum from three replicates for every drying point was used for further computations. It is noteworthy that dark images were taken by closing the shutter to take the sensor noise into consideration.

### 2.6 | Image processing and visualization

All image processing was performed using an in-house software developed in Matlab (version R2020a, MathWorks, USA). First, the

hypercube channels were searched in a loop to find a channel generating the highest contrast between the objects and background. The channel was binarized using Otsu's algorithm and all objects were labeled from top to bottom. Then, the captured images were corrected according to Equation 2:

$$R(\lambda_{xy}) = \frac{I(\lambda_{xy}) - MDN_{\lambda}}{W(\lambda_{xy}) - MDN_{\lambda}} \quad (2)$$

where  $R(\lambda_{xy})$  is the adjusted relative reflectance image,  $I(\lambda_{xy})$  is the original image of the samples,  $W(\lambda_{xy})$  is the image of white tile, and  $MDN_{\lambda}$  is the dark image. Next, the average reflectance spectrum for each carrot slice was calculated. Since lower emissions of the halogen bulbs were observed at the range between 400 and 500 nm, the spectral range from 500.55 to 1010 was used in the PLSR development. Visualization of selected quality attributes was computed by inserting the corresponding spectrum for each pixel into the developed model in order to generate a 2D visualized mapping according to the location of all the corresponding pixels of the carrot slice.

## 2.7 | Multivariate analysis

Partial Least Square Regression (PLSR) was employed for the multivariate analysis by imported all the data sets into JMP software (SAS Institute Inc., Cary, NC, USA). PLSR was used in this study due to its ability to analyze data with numerous noises, collinear, and even incomplete variables in both sample spectrum and reference values (Wold et al., 2001). Carrots from the same variety of Laguna which had grown and harvested in two seasons (2017 & 2018) were combined into one data set regardless of drying treatments, temperature, and thickness in order to develop a robust and independent model. Then, the spectral reflectance for each drying point was averaged from three replicates in order to improve the modeling performance with better accuracy. The methodological approach in this study is simplified as depicted in the flowchart in Figure 2. All variables were preprocessed using mean centering and autoscaling methods before further modeling. Mean centering is the first stage in preprocessing of multivariate methods especially for spectral data in food (Sena et al., 2017). This technique eliminates the mean spectra and shifts the natural data origin to the multivariate mean. Mean centering also ensures that the results are excellent in terms of variation around the mean (Nicolai et al., 2007). Then, the average of each column is computed and then subtracted from each variable (Li et al., 2018). Thus, each mean-centered column has an average of zero. Meanwhile, autoscaling is another primary preprocessing method which includes mean centering and each value is divided by its respective column standard deviation after the subtraction of the column average. Thus, the mean and unit variance in all columns is zero (Sena et al., 2017). Later on, a predictive PLSR model was computed and developed through the nonlinear iterative partial least squares (NIPALS) algorithm with a testing number of factors equal to 15. The same spectral data set with all the quality attributes (total carotenoids, moisture

content,  $L^*$ ,  $a^*$ , and  $b^*$ ) were applied to the protocols so that all quality parameters can be estimated in the future from the measured spectra. The frequency distribution of variables was displayed in the histogram and the data were compressed over the intensities in the bin in order to define the adequate experimental space. The bins were selected based on a fixed width or with an increasing width with an almost equal distribution of data set. The binning process deviates the linear order between the original quantitative values and permits any form of correlation between responses (X) and Y that needs to be modeled (Smolinska et al., 2012). A binning with 10 data splits was optimized for each model and the regression models were computed by applying the two-way cross-validation method in order to resolve the dependency between the predicted error for new individuals and the optimization of the model parameter. The data sets were chosen randomly and divided into two categories of which 60% were used for training and 40% for the validation test. Additional independent data were reserved for testing the model performance. Fully cross-validated PLSR with an optimum number of latent factors was applied to construct a robust model in order to obtain the best prediction results for each quality parameter that is, total carotenoids, moisture content (% wb), and color attributes of  $L^*$ ,  $a^*$ , and  $b^*$ . After that, single cross-validation was carried out on both validation and training sets. The optimal number of PLSR components and the minimum predicted residual error sum of square (PRESS) of the validation set were selected for the optimal number of latent variables (LV) or factors for the PLSR model (Sawatsky et al., 2016). PRESS is calculated based on the sum of squares of deviation between predicted and reference values of quality parameters and was calculated using Equation (3) (Shrestha et al., 2019). This model contains the predicted formula which was performed on both training and validation data sets including the independent test set. The calibration model was applied to predict the independent test data sets. The performance of the model and its accuracy were selected based on the minimum coefficient of determination ( $R^2$ ) and root mean square error (RMSE) for the training set ( $R^2_T$  and  $RMSE_T$ ) and cross-validation set ( $R^2_V$  and  $RMSE_V$ ). The  $R^2$  and RMSE were defined in Equations (4), (5), and (6), respectively (Chai & Draxler, 2014).

$$PRESS = \sum (y_{cal} - y_{act})^2 \quad (3)$$

$$R^2 = 1 - \frac{\sum (Y_{cal} - Y_{act})^2}{\sum (Y_{cal} - Y_{mean})^2} \quad (4)$$

$$RMSE_{CV} = \sqrt{\frac{\sum (Y_{cal} - Y_{act})^2}{n}} \quad (5)$$

$$RMSE_T = \sqrt{\frac{\sum (Y_{pred} - Y_{act})^2}{n}} \quad (6)$$

where  $n$  is the number of spectra (samples),  $y_{act}$  is the actual value,  $y_{mean}$  is mean value,  $y_{cal}$  is the estimated value from calibration model,  $y_{pred}$  is the predicted value of the quality attributes (total carotenoids,



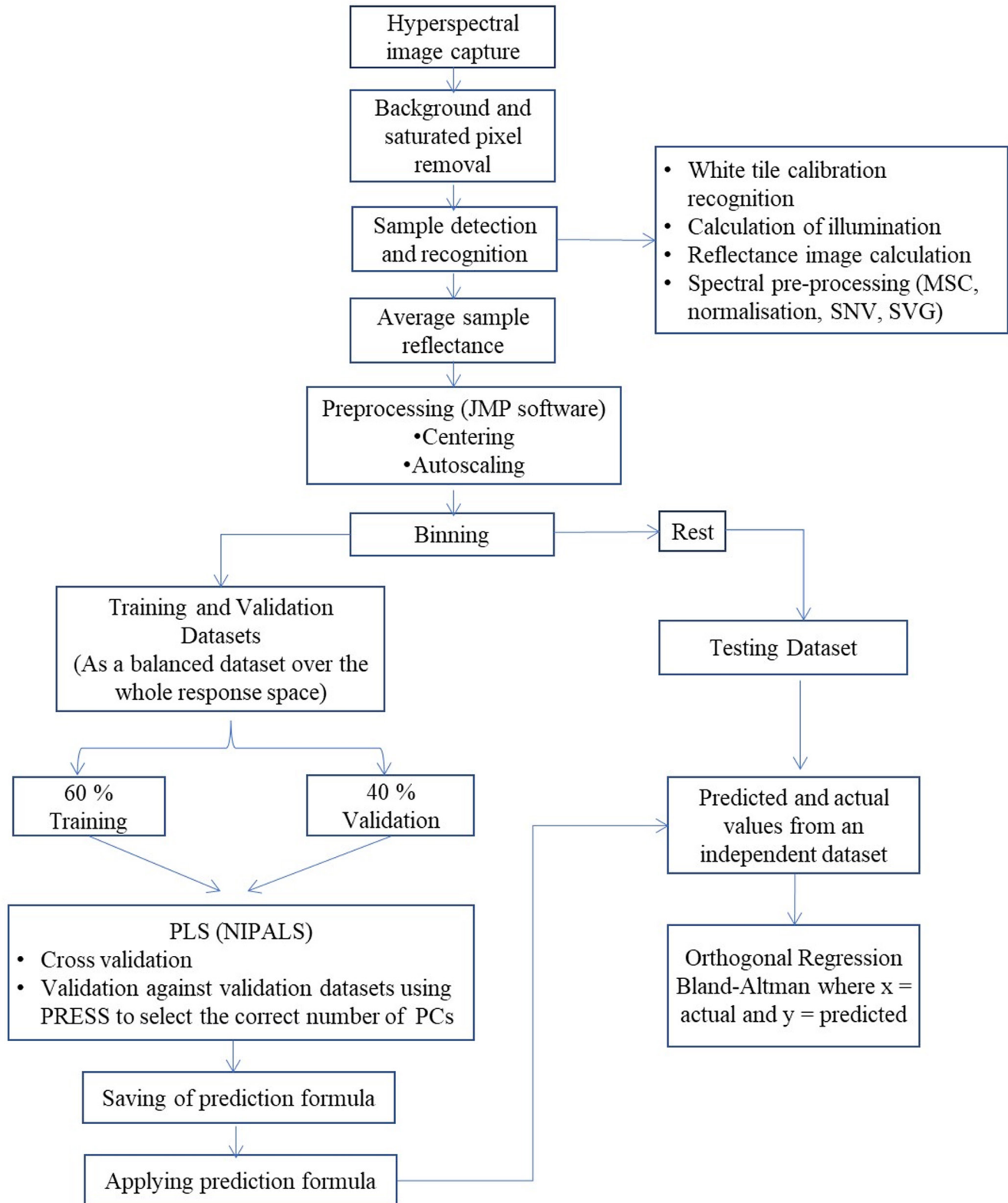


FIGURE 2 Similar methodology approach for each hyperspectral image and data processing adapted from Shrestha et al. (2019)

moisture content,  $L^*$ ,  $a^*$ , and  $b^*$ ) in carrots evaluated by the validation method. The statistical parameters such as  $R^2$  and RMSE which were obtained from the training, validation, and testing data sets were used to assess the quality of the model and to evaluate the influences of

the predictors. The most accurate model was selected based on high  $R^2$  and low RMSE values. The most important wavelengths from the spectral data corresponding to each quality parameter were selected manually based upon loading weights of the Variable Importance in

Projection (VIP) plot from the PLSR models which calculated as the weighted sum of squares of PLS weights. Then, the most significant wavebands that are highly relevant to the quality attributes were identified based on the highest score of the VIP plot (Meacham-Hensold et al., 2020; Shrestha et al., 2019; Amjad et al., 2018; Pu & Sun, 2016). The VIP scores generated from the PLSR can be used to select the most significant variables or predictors. The VIP score for  $j_{th}$  X-variable can be calculated from Equation (7)

$$V_{j=\sqrt{p}} \sum_{a=1}^A SS_a \left( \frac{W_{aj}}{W_a} \right)^2 \quad (7)$$

where  $p$  is the total number of variables,  $A$  is the total number of components,  $SS_a$  is the sum of squares explained by the  $a_{th}$  component,  $SST$  is the total variance explained by all the components, which is computed using loading weight vectors  $W_{aj}$  for each component and  $(W_{aj}/W_a)^2$  indicates the importance of the variable  $j$  for component  $a$ . The VIP score for the predictor variable which is greater than 0.8 is considered as an important variable in this study considering the average squared VIP score (Shrestha et al., 2019; Jun et al., 2009).

## 2.8 | Methods comparison

The Bland–Altman (BA) analysis, Passing–Bablok (PBR), and Deming regression (DR) were used as a method comparison in this study for assessing the agreement between the destructive laboratory method and non-destructive HSI technique for all quality parameters. The BA method is expressed as 95% agreement limits, that is, determined by mean difference  $\pm 1.96$  standard deviations and these values describe the range within which most differences will exist between the two methods. Therefore, the smaller the range between these two limits the better is the agreement between the two methods (Carkeet & Goh, 2018). The aim of BA analysis was to identify and assess significant trends in the graph which can be either a constant bias or a nonconstant bias as well as variance heterogeneities (Bland & Altman, 1999; Carkeet & Goh, 2018). A graphical plot with scattered data points around the regression line with an ideal value of slope equals 1 and an intercept equals to zero (0) will be displayed after computation in PBR. However, the experimental results can divert from the ideal values in various ways (Shrestha et al., 2019). So the test method's bias can be measured by the difference between the regression line (fitting line) and the equality line ( $y = x$ ). The linear regression analysis technique of PBR was also used to estimate the agreement of the analytical methods and to detect possible systematic bias between both measuring methods which is a statistical and nonparametric test procedure (Arendse et al., 2018). The basic principle of the DR (Orthogonal) technique is fitting a straight line to two-dimensional data where both variables,  $X$  and  $Y$ , are measured with error which are proportional to the overall average value of the test and comparative results for each sample (Sârbu et al., 2000).

## 3 | RESULTS AND DISCUSSION

### 3.1 | Multivariate analysis of partial Least Square regression (PLSR)

Figure 3 and Table 1 show statistical parameters with satisfactory prediction accuracy of  $R^2$  for both validation and training sets for all quality attributes. The results obtained indicate substantial variations for each individual slices leading to an acceptable measurement accuracy. These divergences might be attributed to irregular shapes and size of each slice such as severe shrinkage, curvature, and folded surface at certain drying points resulting in varying degree of physical disfiguration of carrot slices causing light dispersion and finally resulting in spectral deviations.

It was also reported that light scattering greatly depended on the physical properties of the produce's tissue (Udomkun et al., 2014). Moreover, high variability of physical characteristics in food materials will reduce prediction accuracy because it will directly impact the optical properties, lightness distribution as well as interaction behaviors with incident light (Zhang et al., 2018). An acceptable statistical performance from the data sets was observed with satisfactory values of  $R^2_T$  for training set at 0.74, 0.92, 0.78 and 0.77, and  $R^2_V$  for the validation set at 0.64, 0.90, 0.68, and 0.69 for total carotenoid, moisture content,  $L^*$  and  $a^*$ , respectively (Table 1). A strong correlation to predict moisture content between the two methods was observed in this study with a high coefficient of determination ( $R^2$ ) of more than 0.9 for both data sets (Table 1). Similar results were obtained by Elmasry et al. (2007). The authors reported identical values of  $R^2$  at 0.90 when evaluating moisture content in strawberries during ripening. An acceptable prediction accuracy of total carotenoids was also observed in this study with a value of  $R^2_T$  at 0.74 and  $R^2_V$  at 0.64 (Table 1) which is comparable to previous result reported by Rungpichayapichet et al. (2015) on the prediction of  $\beta$ -carotene content in mangoes during ripening. The authors reported an  $R^2$  at 0.64 and 0.84 with standard errors of prediction at 20.81 and 14.61 for both calibration and validation data sets when the samples were subjected to a long wave of NIR at 1000–2500 nm. Other nutrients such as vitamin C in different varieties of apples also showed a similar trend with a value of  $R^2$  at 0.8 when using NIR spectroscopy in the region between 400 and 2500 nm (Pissard et al., 2013). In this present study, low  $R^2$  at 0.67 and 0.59 were observed for the color parameter  $b^*$  for both training and validation data sets which indicate an error might occur from both measuring methods due to curvature or glossiness of the sample's surface (van Roy et al., 2017). It was also mentioned that the curve surface of fruits and vegetables will cause uneven light distribution leading to variability in spectral absorbance and finally affecting the prediction accuracy of chemometrics models (Zhang et al., 2015). Nonuniform color distribution during drying also impacts visible differences in appearance and texture that could trigger the irregularity in spectrum pattern since color changes during drying were not homogeneous (Fernandez et al., 2005). Similar results were also obtained by van Roy et al. (2017) and Larrain et al. (2008) on the color parameter of  $b^*$  for tomato and beef

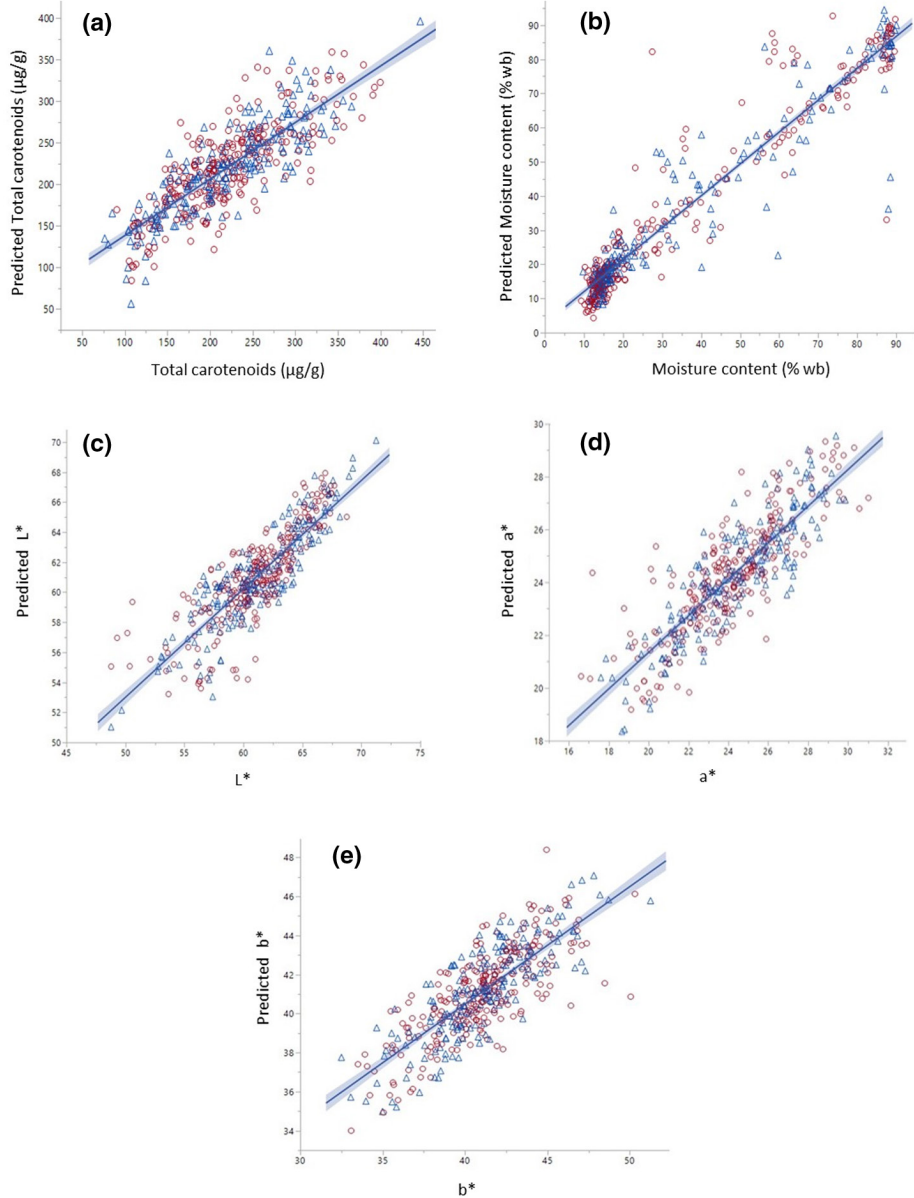


**FIGURE 3** Scatter plot of total carotenoids (a), moisture content (b),  $L^*$  (c),  $a^*$  (d), and  $b^*$  (e) using training (red) and validation (blue) set of carrot samples as predicted by PLSR model and as measured in the laboratory

by using hyperspectral imaging and digital imaging with low  $R^2$  at 0.42 and 0.56, respectively. Furthermore, irregular sample surface, size, and geometry also influence the reflectance variability especially if the window or sensor of the instrument is not completely cover the product surface leading to inaccurate color measurements (van Roy et al., 2017). Minimal values of  $\text{RMSE}_T$  and  $\text{RMSE}_V$  for both data sets were also observed for moisture content,  $L^*$ ,  $a^*$ , and  $b^*$  at 8.15, 1.56, 1.06, and 1.40 for training set, and 8.16, 1.75, 1.18, and 1.45 for validation set, respectively. It was noted that a large range of  $\text{RMSE}_T$  and  $\text{RMSE}_V$  at 28.68 and 32.62 were observed for total carotenoids in both data sets as compared with other quality attributes (Table 1). The results suggest high variation of total carotenoids due to different levels of thermal degradation during drying and vast measurement errors leading to a wide range of total carotenoids

concentration across the whole data sets. A similar trend was also reported by Ihsan et al. (2019) on high RMSE at 39.21 for carotenoids content in apple leaves using hyperspectral imaging with a range of wavelength from 400 to 1000 nm. Moreover, high variation in spectral reflectance related to total carotenoids can be caused by scattering effects of the tissue and consequently impacting the spectral intensities (Zude et al., 2007). Furthermore, the large variations of total carotenoids in this study might be due to the heterogeneity of total carotenoids for each slice because of different harvesting seasons and years since the nutritional compounds of carrot were reported to vary with season (Horvitz et al., 2004) and environmental conditions (Rosenfeld et al., 1998). In addition, different drying strategies from two different drying experiments in this study also caused varying degree of total carotenoids degradation since it was



TABLE 1 Statistical parameters of PLSR modelling and selected wavelengths for quality attributes in carrots

Quality parameters	Statistical parameters and selected wavelengths					Selected wavelengths based on VIP scores
	Calibration		Validation		Root MeanPRESS	
	$R^2_T$	RMSE <sub>T</sub>	$R^2_v$	RMSE <sub>v</sub>		
$L^*$	0.78	1.56	0.68	1.75	0.63	531, 592, 654, 685, 960, 980
$a^*$	0.77	1.06	0.69	1.18	0.57	531, 600, 624, 660, 685, 975
$b^*$	0.67	1.40	0.60	1.45	0.77	531, 592, 629, 650, 680, 960
Moisture content (% wb)	0.92	8.15	0.90	8.16	0.32	531, 585, 973
Total carotenoids ( $\mu\text{g/g}$ )	0.74	28.68	0.64	32.62	0.61	531, 598.97, 623, 654.03, 685, 970

Abbreviations:  $R^2_T$ , Coefficient of determination for training set;  $R^2_v$ , Coefficient of determination for validation set; RMSE<sub>T</sub>, Root Mean Square Error for training set; RMSE<sub>v</sub>, Root Mean Square Error for validation set; Root Mean PRESS, Root Mean of Predicted Residual Sum of Squares.

mentioned that different drying techniques will strongly influence the decomposition of carotenoids (Cui et al., 2004),

Table 1 and Figure 4 present optimum latent variables of 14, 15, 14, 13, and 15 with the least Root Mean PRESS at 0.61, 0.32, 0.63, 0.57, and 0.77 for total carotenoids, moisture content,  $L^*$ ,  $a^*$ , and  $b^*$ , respectively. The number of latent factors with the least PRESS values was selected in this study according to Shrestha et al. (2019) and Khodabakhshian et al. (2017). These factors were chosen in order to prevent overfitting of the data due to choosing too many latent variables or inadequate fraction of training and testing data sets and also underfitting caused by selecting a low number of variables (Shrestha et al., 2019). Thereby, these optimal factors were sufficient for capturing and modeling the data variability. The respective latent factors in PLSR were employed for simultaneous identification of the analytes using the validation method across all the spectral data. It is also possible to analyze the interrelation between quality attributes in order to relate the interaction between quality parameters that could influence the spectral pattern as reported by Schmilovitch et al. (2014). The authors observed a satisfactory level of  $R^2$  at 0.70 for the interaction between total soluble solids and total carotenoids which indicates the possibility to apply HSI with the consideration to oversee the correlation between relevant qualities attributes. In this study, the excellent prediction accuracy of  $R^2$  at 0.85 and low Root mean PRESS at 0.47 were obtained when two responses of total carotenoids and moisture content were analyzed together showing a significant correlation between these two variables during the drying process. The results were confirmed by our previous work on the influence of moisture content on total carotenoids retention during drying (Md Saleh et al., 2019). There is also a possible interaction between color parameter  $a^*$  with both moisture content and total carotenoids in carrots during drying which shows a good correlation of  $R^2$  at 0.76 with low Root mean PRESS value at 0.52 (Table 2). However, a moderate correlation of  $R^2$  between  $a^*$  and total carotenoids was observed at 0.69 with a slightly higher value of Root mean PRESS at 0.58. The above computed outputs from PLSR modeling provide encouraging results with useful information on the possibility to apply non-invasive quality measurements to facilitate the online monitoring of the drying process. However, continuous method improvements must be carried out before it can be

implemented into practical applications since considerable variability of resulting spectra for each individual slice was observed in this study, indicating a challenging task for upgrading and refining both procedures along the processing chain.

All aspects of quality management need to be optimized and standardized starting from the preparation of the raw material to the end products with a constant development of a new simplified algorithm for efficient and reliable data extraction, processing, and computation since all variations greatly depend on instrumental noise, complex chemical composition of products, environmental factors, and other sources of variations that can complicate the resulting spectrum (Li et al., 2018; Liu et al., 2015).

### 3.2 | Analysis of spectral reflectance and wavelength selection based on VIP plot

The average spectral reflectance of carrots over the range of wavelength from 400 to 1010 nm at different time points of the drying process is shown in Figure 5. Similar trends of spectra were observed for all measurement points indicating consistent changes of reflectance throughout the drying process. Lower reflectance intensities were observed in fresh samples in the regions between 500 to 540 nm and 900 to 980 nm. However, the reflectance values increased with an increase in drying time due to degradation of total carotenoids and reduction of moisture content. This is due to the fact that both regions correspond to total carotenoids and moisture content absorption peaks (Chaudhry et al., 2018; Liu et al., 2016). Changes in spectral reflectance in both regions during drying are related to the decomposition of color and changes in chemical compositions due to thermal damage of total carotenoids and moisture losses during drying. Furthermore, changes in spectral reflectance are caused by changes in absorption and scattering properties of fruits and vegetables during drying. These changes are influenced by physico-chemical transformations of chemical components, hardness, microstructure, and texture of the products which are induced by process conditions during convective drying (Mozaffari et al., 2016). According to Mozaffari et al. (2016), changes in spectral profile of laser backscattering imaging during drying of apples were

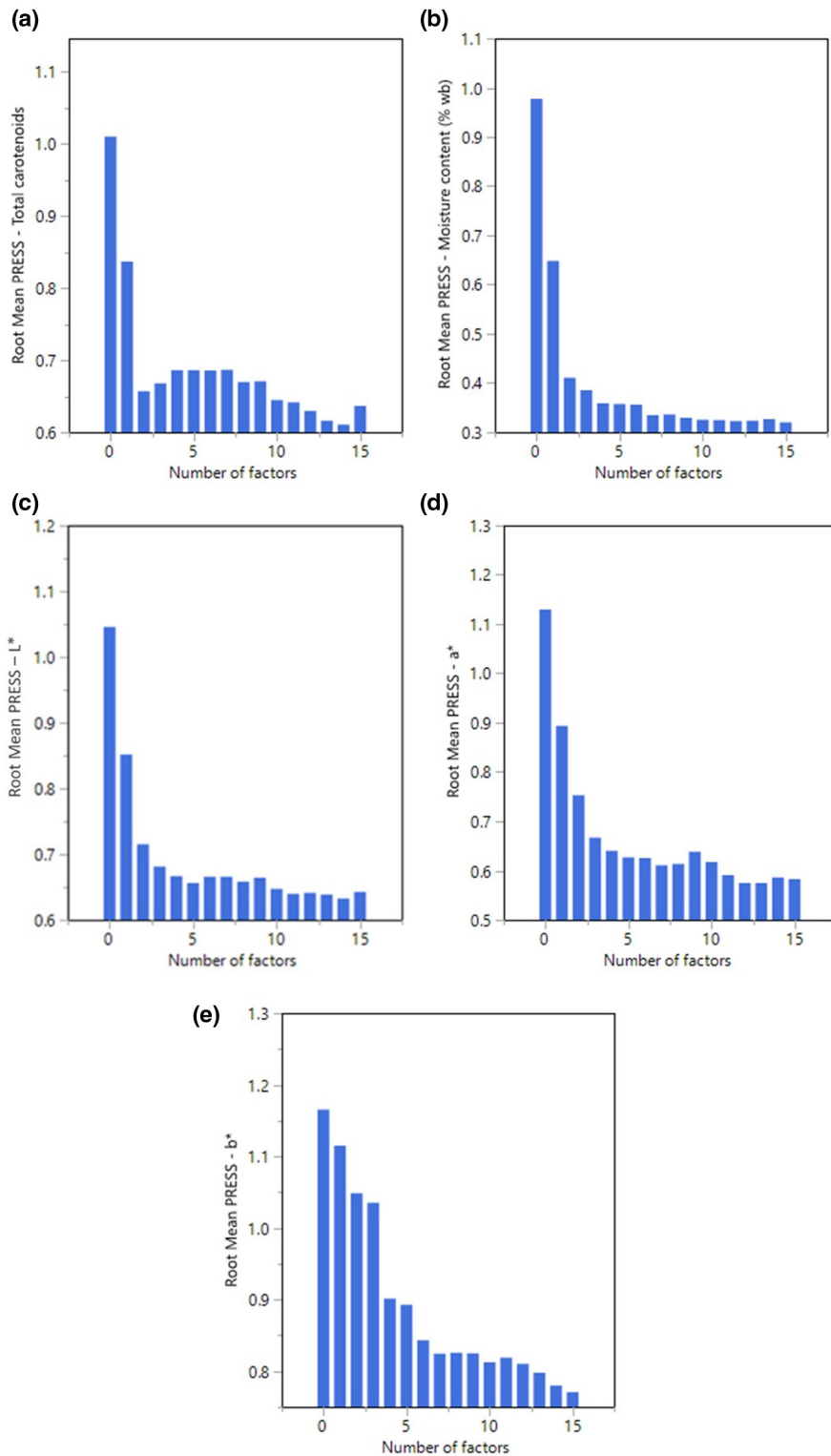


FIGURE 4 Predicted residual errors sum of squares (PRESS) plot for (a) total carotenoids, (b) moisture content (% wb), (c)  $L^*$ , (d)  $a^*$ , and (e)  $b^*$  as a function of a number of factors in dried carrot

closely related to enzymatic oxidation, nonenzymatic browning as well as degradation of color and carotenoids. In the case of carrots, any noticeable changes in color can be correlated with degradation of total carotenoids and nonenzymatic browning (Koca et al., 2007). Therefore, changes in the spectral pattern can be a potential indicator to predict both color and total carotenoids transformation and the application of non-invasive quality evaluation using HSI is

helpful for evaluating the dynamic changes during drying without interrupting the process.

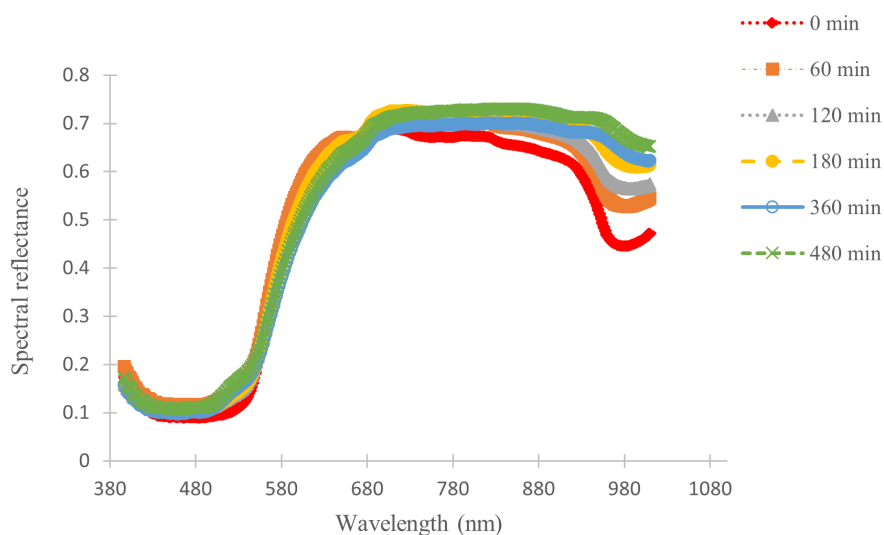
The VIP plots of total carotenoids, moisture content (%wb),  $L^*$ ,  $a^*$ , and  $b^*$  of carrots at 323 wavelengths from 500.55 to 1006.58 nm are displayed as in Figure 6. In this study, any wavelengths with a VIP score of more than 0.8 are considered as an important and significant wavelength for quality prediction (Shrestha et al., 2020).

**TABLE 2** Statistical parameters of PLSR modelling for interaction between quality attributes

Quality parameters	Statistical parameters	
	R <sup>2</sup>	Root Mean PRESS
Interaction between moisture content (% wb) and total carotenoids	0.85	0.47
Interaction between <i>a</i> * and total carotenoids	0.69	0.58
Interaction between <i>a</i> *, moisture content and total carotenoids	0.76	0.52

Abbreviations: R<sup>2</sup>, Coefficient of determination; Root Mean PRESS, Root Mean of Predicted Residual Sum of Squares.

**FIGURE 5** Average spectral reflectance of carrots at different drying time



VIP plots also indicate which X variables (wavelengths) had the most influence on a model. The most influential wavelengths which correspond to the quality attributes of carrots were selected based on the highest loading of VIP scores in this study. It was found that the highest peak of spectral reflectance was dominant at certain wavelengths displaying different spectral signatures for specific quality attributes. Figure 6 (a) and Table 1 show noticeable peaks at the wavelength between 520 to 545 nm and the highest peak in that region was observed at 531 nm which can be attributed to total carotenoids content (Haas et al., 2019). A spike of peaks in the wavelength regions between 500.55 and 685.71 nm is illustrated in Figure 6c–e which might be related to color of carrots as denoted by the color parameters of *L*\*, *a*\* and *b*\*. The highest peak for *L*\*, *a*\*, and *b*\* were observed at 531, 531, and 680 nm, respectively, which might be related to chlorophyll “a” in carrots (Zude et al., 2008). It was reported that wavelength peaks from the region of 430–670 nm correspond to Chlorophyll a, and from 460 to 640 nm to Chlorophyll b. The range of carotenoid peaks was observed from the region from 470 to 530 nm (Chaudhry et al., 2018). So, the selected wavelengths obtained in this study for total carotenoids and color were close and within the particular regions as reported in the previous literatures.

An apparent peak in the region between 959.11 to 985.26 was observed in VIP plot for moisture content with the highest peak spikes at 973 nm (Figure 6b and Table 1). The corresponding wavelength was related to moisture content due to the strong absorption

of infrared radiation by water and the engagement of hydrogen bonds with one or two OH groups within a NIR spectrum between 730 and 2300 nm which in turn will influence the NIR absorption (Yu et al., 2019; Amodio et al., 2017). This noticeable peak was also associated with the stretching of the H–O–H bonds within water molecules and the prominent absorption peak for water was reported to be around 970 nm (Sturm et al., 2020; Kandpal et al., 2013).

### 3.3 | Predictive ability of PLSR model and method comparison based on Passing–Bablok and Deming regressions

The statistical comparison between two methods in analytical chemistry is the most crucial step in method validation and the task is usually completed by employing a regression technique for method comparisons (Mocák et al., 2003). In our study, the results obtained from laboratory methods are considered as a reference method or gold standard and it will be plotted horizontally on the X axis and the predicted results acquired from HSI are plotted on the Y axis (Figure 7). The data set is strictly paired. The equality line is displayed as a dotted gray line with a slope of 1 and an intercept of 0. Statistically, the two methods would have a 100% agreement if all observed points were set on this line with a R<sup>2</sup> equal to 1 which is unlikely to happen in a real situation since no measurement

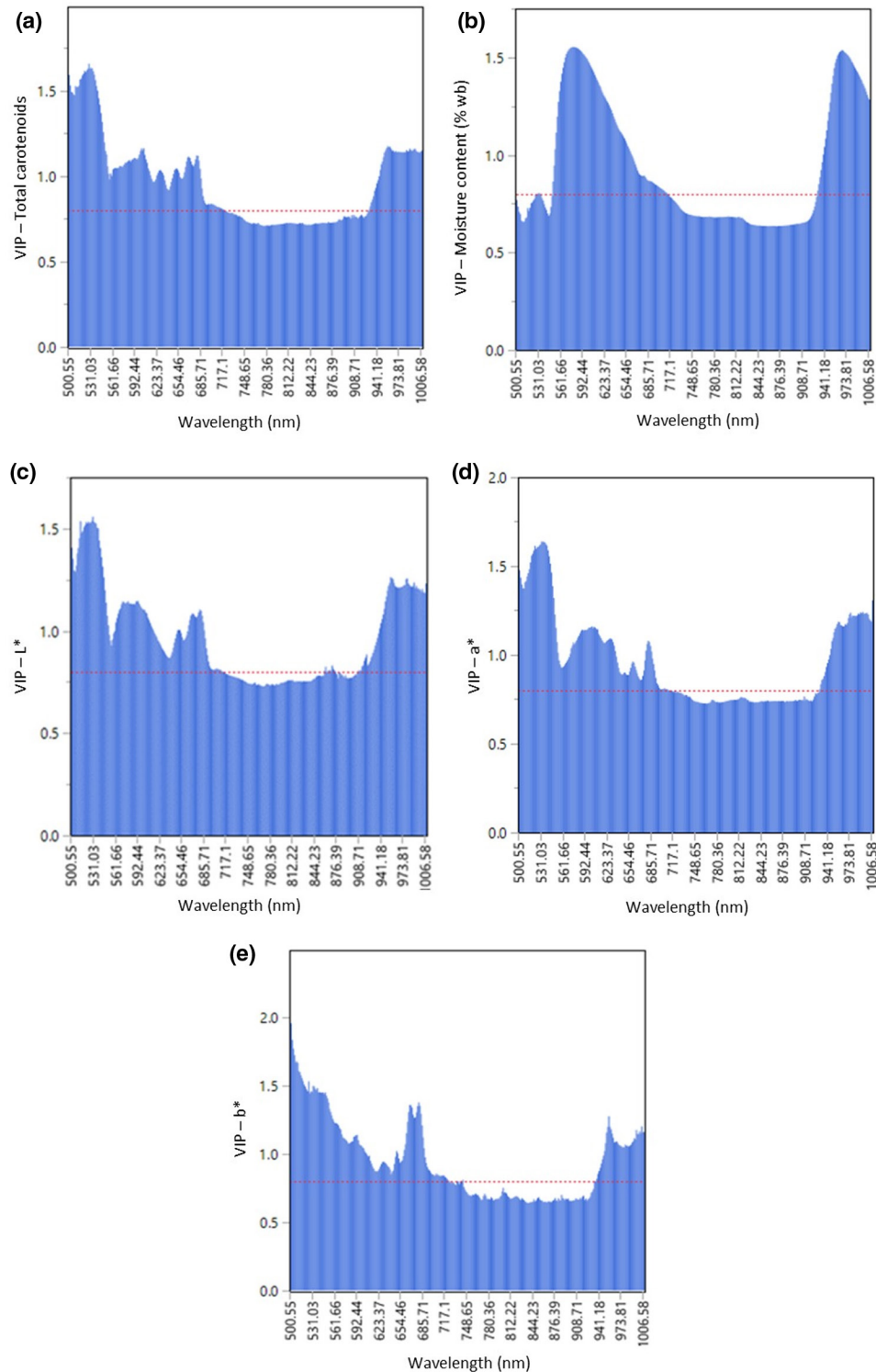


**FIGURE 6** Variable importance projection (VIP) plots for total carotenoids, moisture content (% wb),  $L^*$ ,  $a^*$ , and  $b^*$  at wavelengths between 500.55 and 1006.58 nm

methods are perfect (Ludbrook, 2010). The DR (red line) and the PBR (blue line) were evaluated simultaneously. A random scattering patterns around the equality line were observed between measured and predicted values of total carotenoids, moisture content (% wb),  $L^*$ ,  $a^*$ , and  $b^*$  which indicates that there is a discrepancy between the methods. However, the values of concordance

correlation coefficient ( $r$ ) from DR are 0.69, 0.89, 0.91, 0.78, and 0.83 for total carotenoids, moisture content (% wb),  $L^*$ ,  $a^*$ , and  $b^*$ , respectively, which indicate satisfactory correlations between the two compared methods for moisture content and color but a moderate predictive performance for total carotenoids. This is in accordance with findings of other researchers since it is a great

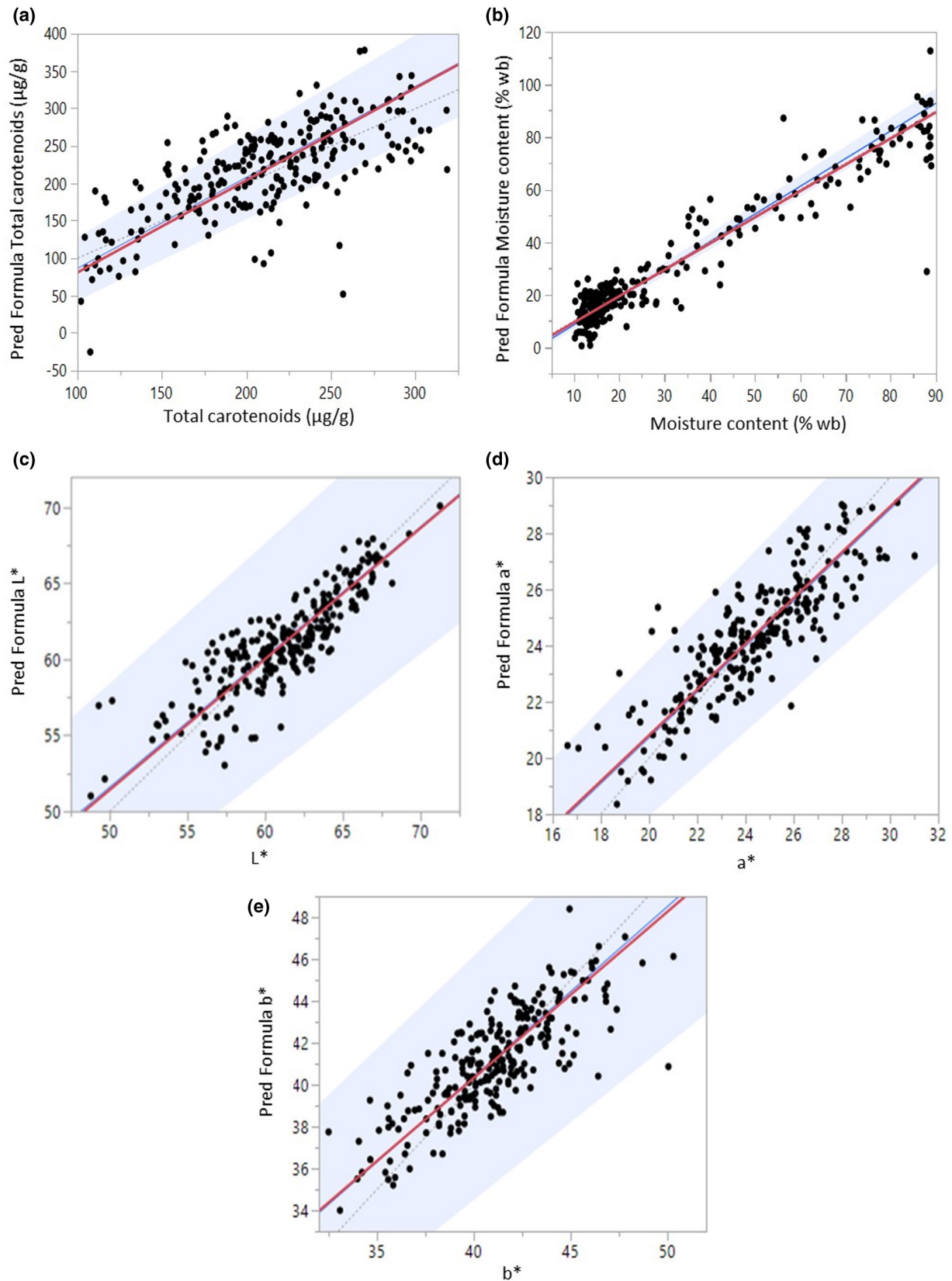


**FIGURE 7** Regression analysis of quality parameters of carrots (total carotenoids (a), moisture content (% wb) (b),  $L^*$  (c),  $a^*$  (d), and  $b^*$  (e)) predicted by PLSR versus measured values of laboratory methods. The dashed gray line: A line of equality, solid red line: A result of the Deming regression with the obtained fit ratio, solid blue line: A line of Passing-Bablok regression



challenge to accurately predict the internal quality of fruits and vegetables using hyperspectral imaging (Lu et al., 2017). However, a good agreement between these two methods was observed at medium concentrations of total carotenoids around 180  $\mu\text{g/g}$  to 260  $\mu\text{g/g}$  with almost an equal scattered distribution from both sides of the equality line (Figure 7a). This is because, at that concentration, most of the carrot slices still contained substantial amounts of moisture (MC >30%) and they were still in a good shape with low levels of shrinkage and minor physical deformation resulting in better light absorption into the materials. It was also testified that the reduction of moisture content in apples during hot air drying caused changes in absorption and scattering properties of the product due to structural modification of the tissue such as changes in size, density, and food matrix (Mozaffari et al., 2016; Udomkun et al., 2014). The results signify that, minimal physical deformation in carrots results in lower light scattering incidence which leads to a good prediction of total carotenoids by using HSI. The same pattern of observation based on DR was also reported by Chen et al. (2013) on insulin detection by two different methods. The authors indicated a good agreement between the two methods was observed at lower concentrations of insulin which implied that the measurements from both methods from the previous study can be in a good agreements to some extent or as in our case of carrots drying, there is a limitation at which the new method of HSI can be reliable at a certain range of total carotenoids concentrations and moisture levels since a good agreement for both methods was observed at higher moisture contents (>30%). Additionally, the simultaneous response and interference from other compounds which occur in parallel with dynamic changes from a combination of multi chemical components in food during drying will influence the reflectance performance resulting in spectral variation and overlapping in the spectral regions, thus leading to complicated spectra (Li et al., 2013). Moreover, heterogeneity of physical and biological properties of agricultural products greatly influences their optical propagation properties and interaction behaviors with incident light, thus reducing the accuracy of quality measurements (Zhang et al., 2018). The same observations of low coefficient of determination at less than 0.20 were also reported on sucrose prediction by HSI in wheat kernels (Delwiche et al., 2013).

The computed results from both regression methods in this study show the slopes and intercepts of PBR and DR regressions as in Table 3 are not confidently different from 1 and 0 for all quality parameters with orthogonal fit ratios of 1.52, 0.99, 0.81, 0.54, and 0.52 for total carotenoids, moisture content (% wb),  $L^*$ ,  $a^*$ , and  $b^*$ , respectively. The observed orthogonal fit ratios which differ from an ideal value of 1 imply that both measuring techniques possess different measurement uncertainties due to analytical errors, seasonal variations, or environmental conditions that could possibly contribute to quality variations for each root and finally influence the measured values (Shrestha et al., 2020; Ludbrook, 2010). A proportional and systematic difference (or BIAS) between the laboratory analysis and the HSI method was not observed in this study since both intercepts and slopes are confidently different from 0 and 1. The above results from both regression techniques indicate an acceptable agreement between the pairs of measurement methods which suggest that in each case both techniques can be potentially applied interchangeably for rapid prediction of total carotenoids, moisture content (% wb), and color parameters of  $L^*$ ,  $a^*$ , and  $b^*$  in carrots during drying.

### 3.4 | Bland–Altman plot analysis for verifying the limit of agreement between two methods

The Bland–Altman plot as in Figure 8 was analyzed based on the differences and agreement between the predicted values (by PLSR) and measured values (laboratory method) for total carotenoids, moisture content (% wb),  $L^*$ ,  $a^*$ , and  $b^*$  against the mean of both methods. The outcomes from the plot show an acceptable agreement between the compared methods with a relatively small mean of difference of 6.67 and a standard error of 2.94 with a satisfactory correlation of “r” equal to 0.69 for total carotenoids (Figure 8 and Table 4). A few outliers were detected in the plot which indicates samples heterogeneities due to biological, seasonal, and environmental variations that could influence the initial concentration of total carotenoids since it was observed that the amount of total carotenoids in this experiment varied for each individual root. The measurement errors and physical distortion of each individual slices could also contribute to spectral variation and finally lead to extreme measurement

Variable	Variance fit ratio	r	Slope		Intercept	
			DR	PBR	DR	PBR
Total carotenoids	1.52	0.69	1.23	1.22	-42.33	-35.06
Moisture content (%wb)	0.99	0.89	0.99	1.04	1.24	-0.57
$L^*$	0.81	0.91	0.90	0.85	5.95	9.35
$a^*$	0.54	0.78	0.73	0.73	6.63	6.63
$b^*$	0.52	0.83	0.72	0.74	11.89	11.35

TABLE 3 Regression parameters from Passing Bablok (PBR) and Deming regressions (DR) for method comparisons for total carotenoids, moisture content (%wb),  $L^*$ ,  $a^*$  and  $b^*$  measured by hyperspectral imaging (X) and standard laboratory measurement as a reference method (Y)

Abbreviations: DR, Deming regression; PBR, Passing-Bablok regression; r, coefficient of correlation.

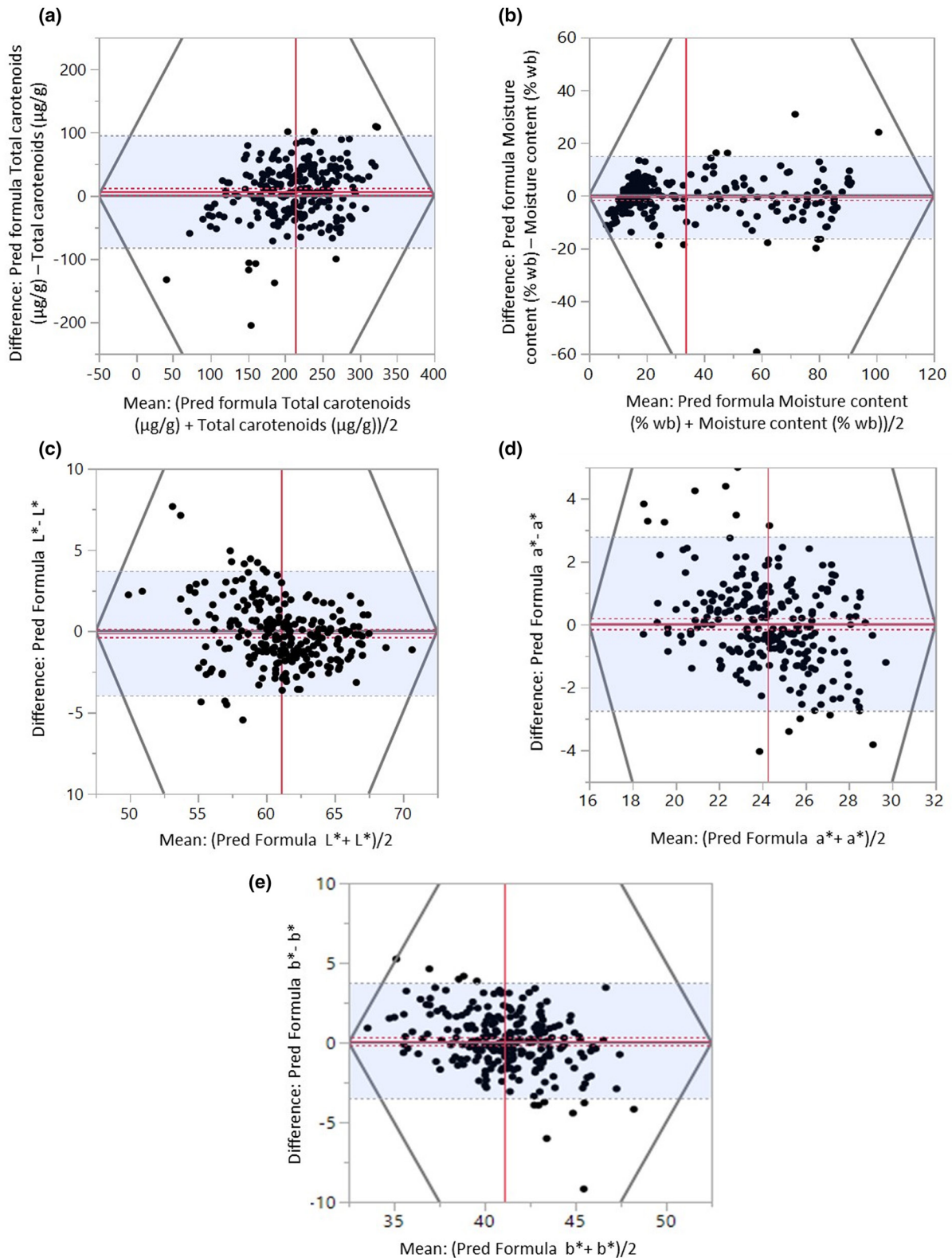


**FIGURE 8** Bland-Altman plots for quality parameters in carrots which show the differences between predicted and measured values vs the mean value of both measurements. Dashed gray lines indicate the limit of agreement ( $\pm 1.96$  S.D of difference), the solid black line is the line of equality, the solid red line shows the mean difference (bias), and the dashed red lines show the 95% CI around the mean difference

values and predictions. The BA plot for total carotenoids displays equally distributed points between the limits of agreements at 95% CI which is expanding from 95.68  $\mu\text{g/g}$  to 82.34  $\mu\text{g/g}$  demonstrating

a satisfactory agreement within an acceptable level between non-destructive technique and laboratory analysis (Sedgwick, 2013). In other words, we can say that 95% of the plotted data points would

TABLE 4 Statistical parameters of Blant Altman analysis for quality attributes in carrots

Variable	Upper limit	Lower limit	Mean difference	Standard deviation	Standard error	r
Total carotenoids	95.68	-82.34	6.67	45.41	2.94	0.69
Moisture content (% wb)	25.18	22.93	1.12	7.96	1.92	0.89
$L^*$	2.88	-3.30	-0.21	1.96	0.25	0.91
$a^*$	4.15	-3.43	0.36	1.41	0.36	0.78
$b^*$	4.53	-3.11	0.71	1.85	0.30	0.83

Abbreviation: r, coefficient of correlation.

have a measurement difference within the limits of agreement in the range between 95.68 and 82.34 interval. The wide interval in this study implies that large differences in measurements due to a wide range of total carotenoids retention were observed throughout the drying period. The mean differences for moisture content, color parameters of  $L^*$ ,  $a^*$ , and  $b^*$  are 1.12, -0.21, 0.36, and 0.71, respectively, indicate that both applied methods are evidently comparable and acceptable as the mean difference is approaching toward zero, and the standard deviation of the variations between measurements does not exhibit any systematic variance with the mean of the measurement pairs. Low values of standard deviations at 1.96, 1.41, and 1.85 were observed for the color parameters of  $L^*$ ,  $a^*$ , and  $b^*$  which demonstrate an appropriate agreement between both measurement methods. However, a higher standard deviation for total carotenoids at 45.41  $\mu\text{g/g}$  was obtained in this study due to a broad range of total carotenoids concentration across the data sets implying varying degrees of total carotenoids decomposition when subjected to heat treatment. Previous research which was reported by Rungpichayapichet et al. (2015) also showed similar patterns with higher standard deviation at 36.71 of predicted  $\beta$ -carotene by PLSR model in mango during ripening by employing a non-invasive technique of near-infrared spectroscopy at 700–1100 nm. Nevertheless, an acceptable agreement was achieved for total carotenoids in this study with just 10 outliers from 239 data sets between non-invasive technique and Gold Standard method, implying that only 4.14% of the total carotenoid values surpassed 95% of the acceptability limits. The result obtained complies with the statistical agreement since it is recommended that 95% of the data points should lie within the limits of agreement at  $\pm 1.96$  SD of the mean difference (Earthman, 2015; Sedgwick, 2013). The findings demonstrate the possibility of using non-destructive technique for total carotenoids measurement during drying. For moisture content, a good level of agreement was also observed at a minimal value of standard deviation at 7.96 with only seven outlier points, indicating only 2.93% of the differences in measured values fell outside the 95% acceptability limits. Both findings are within an agreeable statistical limit as described by Bland and Altman (1999). The results also show minor values of standard error at 1.92, 0.25, 0.36, and 0.30 for moisture content,  $L^*$ ,  $a^*$ , and  $b^*$  (Table 4). Therefore, the new HSI technique can be performed interchangeably for non-destructive quality inspection in carrots with an acceptable accuracy as compared with a conventional laboratory method. In view of this, we can suggest that there is a great potential

for adopting the application of HSI for non-invasive assessment of moisture content and color in carrots, despite the fact that both methods could possibly possess their own errors in various ways and the errors could be linked to sampling, sample preparation, and instrumental noise. The errors within laboratory methods can possibly occur at various stages of sample preparation prior to physical and chemical analysis. All these errors will contribute to a significant variation in the measurements (Amodio et al., 2017).

### 3.5 | Visualization of moisture content at different drying periods

Figure 9 shows a mapping of moisture content in carrots at different stages of the drying process at 60°C. The images for samples drying at 60°C were selected due to the best quality retention which is based on our previous study (Md Saleh et al., 2019). The displayed images from Figure 9 demonstrate higher moisture distribution was observed at the center of the carrot slice at the early stage of drying between 90 and 150 min and lower moisture content at the edge of the slices at all stages of drying indicating a higher moisture removal rate at the edge of the surface area. The images also show a significant size reduction as the drying proceed due to water removal during drying and finally leading to physical deformation such as volume shrinkage (Pu & Sun, 2015). Therefore, a bias during measurements occurred due to physical disfiguration of the carrot slice leading to inaccurate mapping predictions. This error was unavoidable and for that reason, higher moisture regions were observed at some spots on the edge of the slice toward the final stage of the drying process. Additionally, Zhang et al. (2018) reported that, the curved surface, shape, size, and color of fruits and vegetables influenced the reflectance components. Furthermore, the authors also mentioned that the curved surface will cause nonuniform reflectance leading to uneven light distribution; especially the zone near to the border resulting in misinterpretation or it can be incorrectly identified as defects. Consequently, the irregular surfaces would promote spectral variability and enhance the complexity of the calibration model and finally reduce the prediction accuracy and practicability of the model. In general, despite of inevitable challenges of variability in physical distortion of each individual slice of carrots, visualization of moisture distribution using HSI during drying is useful for evaluating the performance of the drying process when subjected to different drying

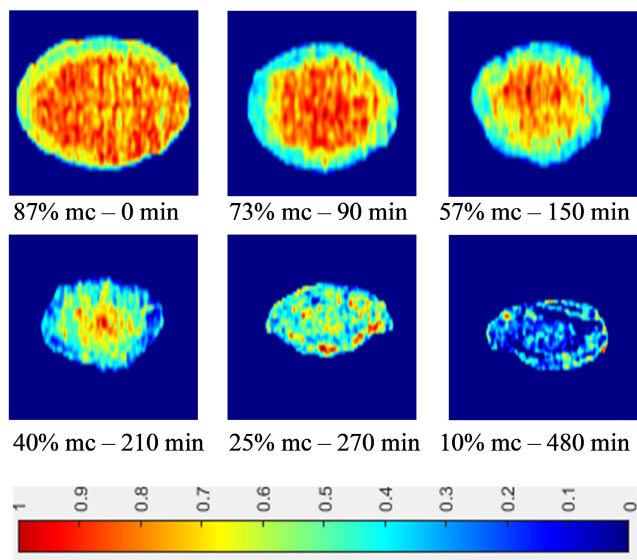


**FIGURE 9** Distribution of moisture content in carrot at different drying period at 60°C

conditions. This advanced technique enables a good prediction of the moisture evolution throughout the whole process, which can be a reliable indicator for determining the optimum drying time on when to stop the drying process and it can be helpful for dynamic optimization of the drying process with regards to product quality and safety.

## 4 | CONCLUSIONS

Hyperspectral imaging combined with chemometrics demonstrates to be a promising technological tool for non-destructive quality measurements during the drying of carrots. An excellent prediction of moisture content in this study indicates the potential usage of this technique for online and real-time quality assessment. This technique also provides the satisfactory prediction of total carotenoids and the color parameters of  $L^*$  and  $a^*$ . Satisfactory results for intercepts and slopes in Passing–Bablok and Deming regressions were obtained with both values approaching 0 and 1 indicating a good statistical agreement between the compared method pairs. The results were confirmed by the Blant–Altman analysis with more than 95% of the measured values were within the 95% CI of the statistical limits for all quality attributes. The findings demonstrate a possibility to apply non-destructive quality measurement using hyperspectral imaging of carrots during drying. This new and innovative method has a great potential to substitute a standard laboratory method in the future. However, it is still a challenging task to accurately quantify total carotenoids in carrots by means of hyperspectral imaging due to the inherent chemical and physical complexities of carrots as well as constant physical changes throughout the drying process that could influence the spectral reflectance and consequently lead to inconsistent predictive values of the actual retention of total carotenoids in carrots. The application of hyperspectral imaging for noncontact and quantification of total carotenoids could provide us with

meaningful information on nutrient degradation at any drying point and rough estimation of nutrient retention based on the changes in spectral reflectance throughout the drying process. Based on this information, adequate drying strategies based on product quality aspects, for example, the inflection point of nutrients degradation, can be performed for effective process control. This study also provides preliminary information toward designing and integrating a non-invasive measurements technique into the drying systems for the development of smart dryers so that, a continuous and online monitoring of quality attributes can be realized and implemented in the future.

## 5 | FUTURE RECOMMENDATIONS

The above study demonstrates the importance of acquiring an in-depth knowledge of optical properties of food crops and their interaction with light as well as the propagation mechanisms of light in the food tissue must be well understood because it can provide relevant information and significant inputs in designing an effective optical system for online and non-invasive quality measurement to control the drying process. Comprehensive studies on the influence of food microstructure on dynamic changes of quality attributes throughout the drying process must be carried out since all these factors contribute to the spectral pattern and prediction accuracy of the resulting outputs from the hyperspectral imaging systems. Multidisciplinary research areas must be scientifically integrated to overcome existing challenges in the understanding of physical, chemical, and biological variability of fruits and vegetables that could cause significant spectral fluctuations and consequently affect the prediction accuracy especially when dealing with samples at different exposure times throughout the processing period such as drying operations. More robust, simple, and reliable algorithms with a universal and practicable calibration models need to be developed which are independent of origins, cultivars, cultivation practices, seasons, and maturity to improve the predictability of future samples.

## ACKNOWLEDGMENTS

The authors gratefully acknowledge the Universität Kassel and Malaysian Agricultural Research & Development Institute (MARDI) for the scientific supervision, PhD scholarship, and financial support. The study is also a part of a research program under the SusOrgPlus project within the framework of the Coordination of European Transnational Research in Organic Food and Farming Systems Cofund Programme and is supported by funds of the Federal Ministry of Food and Agriculture (BMEL) based on a decision of the Parliament of the Federal Republic of Germany via the Federal Office for Agriculture and Food (BLE) under the innovation support program (Project number: BLE – 2817OE005). The work was furthermore supported by the German Research Foundation (DFG-Deutsche Forschungsgemeinschaft) by providing the research funding through the RealTimeFood project (Project number: 420778578). The authors acknowledge the Department of Organic Food Quality and Food Culture, particularly Ms. Gaby Mergardt for



the technical support and provision to access the laboratory and equipment prior to chemical analysis.

## AUTHOR CONTRIBUTIONS

**Rosalizan Md Saleh:** Conceptualization; data curation; formal analysis; investigation; methodology; writing – original draft; writing – review and editing. **Boris Kulig:** Formal analysis; methodology; software; validation. **Arman Arefi:** Data curation; software; validation; writing – review and editing. **Oliver Hensel:** Funding acquisition; project administration; resources; supervision. **Barbara Sturm:** Conceptualization; methodology; resources; supervision; writing – review and editing.

## DATA AVAILABILITY STATEMENT

Research data are not shared.

## ORCID

Rosalizan Md Saleh  <https://orcid.org/0000-0001-5692-4403>

Boris Kulig  <https://orcid.org/0000-0002-7077-9377>

Arman Arefi  <https://orcid.org/0000-0003-1038-6974>

Oliver Hensel  <https://orcid.org/0000-0002-7732-0278>

Barbara Sturm  <https://orcid.org/0000-0002-6269-1906>

## REFERENCES

- Amjad, W., Crichton, S. O., Munir, A., Hensel, O., & Sturm, B. (2018). Hyperspectral imaging for the determination of potato slice moisture content and chromaticity during the convective hot air drying process. *Biosystems Engineering*, 166, 170–183.
- Anonymous. (2002). *Chroma meter CR-400/410 instruction manual*. Konica Minolta Sensing Inc.
- Anunciato, T. P., & da Rocha Filho, P. A. (2012). Carotenoids and polyphenols in nutricosmetics, nutraceuticals, and cosmeceuticals. *Journal of Cosmetic Dermatology*, 11(1), 51–54.
- AOAC. (2012). *AOAC official methods of analysis* (18th ed.). AOAC International.
- Arefi, A., Sturm, B., von Gersdorff, G., Nasirahmadi, A., & Hensel, O. (2021). Vis-NIR hyperspectral imaging along with gaussian process regression to monitor quality attributes of apple slices during drying. *LWT - Food Science and Technology*, 152, 112297. <https://doi.org/10.1016/j.lwt.2021.112297>
- Arendse, E., Fawole, O. A., Magwaza, L. S., Nieuwoudt, H., & Opara, U. L. (2018). Comparing the analytical performance of near and mid infrared spectrometers for evaluating pomegranate juice quality. *LWT - Food Science Technology*, 91, 180–190. <https://doi.org/10.1016/j.lwt.2018.01.035>
- Arscott, S. A., & Tanumihardjo, S. A. (2010). Carrots of many colors provide basic nutrition and bioavailable phytochemicals acting as a functional food. *Comprehensive Reviews in Food Science and Food Safety*, 9(2), 223–239.
- Baek, I., Kusumaningrum, D., Kandpal, L. M., Lohumi, S., Mo, C., Kim, M. S., & Cho, B. K. (2019). Rapid measurement of soybean seed viability using kernel-based multispectral image analysis. *Sensors*, 19(2), 1–16. <https://doi.org/10.3390/s19020271>
- Bilic-Zulle, L. (2011). Comparison of methods: Passing and Bablok regression. *Biochimica Medica*, 21(1), 49–52.
- Bland, J. M., & Altman, D. G. (1999). Measuring agreement in method comparison studies. *Statistical Methods in Medical Research*, 8(2), 135–160. <https://doi.org/10.1191/096228099673819272>
- Bro, R., van den Berg, F., Thybo, A., Andersen, C. M., Jorgensen, B. M., & Andersen, H. (2002). Multivariate data analysis as a tool in advanced quality monitoring in the food production chain. *Trends in Food Science and Technology*, 13(6–7), 235–244.
- Brunsgaard, G., Kidmose, U., Sorensen, L., Kaack, K., & Eggum, B. O. (1994). The influence of variety and growth conditions on the nutritive value of carrots. *Journal of the Science of Food and Agriculture*, 65(2), 163–170. <https://doi.org/10.1002/jsfa.2740650207>
- Carkeet, A., & Goh, Y. T. (2018). Confidence and coverage for Bland–Altman limits of agreement and their approximate confidence intervals. *Statistical Methods in Medical Research*, 27, 1559–1574. <https://doi.org/10.1177/0962280216665419>
- Chai, T., & Draxler, R. R. (2014). Root mean square error (RMSE) or mean absolute error (MAE)?—arguments against avoiding RMSE in the literature. *Geoscientific Model Development*, 7(3), 1247–1250.
- Chaudhry, M. M., Amodio, M. L., Babellahi, F., de Chiara, M. L., Rubio, J. M. A., & Colelli, G. (2018). Hyperspectral imaging and multivariate accelerated shelf life testing (MASLT) approach for determining shelf life of rocket leaves. *Journal of Food Engineering*, 238, 122–133.
- Chen, H. Z., Song, Q. Q., Tang, G. Q., & Xu, L. L. (2014). An optimization strategy for waveband selection in FT-NIR quantitative analysis of corn protein. *Journal of Cereal Science*, 60(3), 595–601.
- Chen, Z., Caulfield, M. P., McPhaul, M. J., Reitz, R. E., Taylor, S. W., & Clarke, N. J. (2013). Quantitative insulin analysis using liquid chromatography-tandem mass spectrometry in a high-throughput clinical laboratory. *Clinical Chemistry*, 59(9), 1349–1356. <https://doi.org/10.1373/clinchem.2012.199794>
- Chong, I. G., & Jun, C. H. (2005). Performance of some variable selection methods when multicollinearity is present. *Chemometrics and Intelligent Laboratory Systems*, 78(1), 103–112.
- Cornbleet, P. J., & Gochman, N. (1979). Incorrect least-squares regression coefficients in method-comparison analysis. *Clinical Chemistry*, 25(3), 432–438.
- Da Silva Dias, J. C. (2014). Nutritional and health benefits of carrots and their seed extracts. *Food and Nutrition Sciences*, 5(22), 2147–2156.
- Delwiche, S. R., Souza, E. J., & Kim, M. S. (2013). Limitations of single kernel near-infrared hyperspectral imaging of soft wheat for milling quality. *Biosystems Engineering*, 115(3), 260–273. <https://doi.org/10.1016/j.biosystemseng.2013.03.015>
- Doğan, N. Ö. (2018). Bland-Altman analysis: A paradigm to understand correlation and agreement. *Turkish Journal of Emergency Medicine*, 18(4), 139–141.
- Earthman, C. P. (2015). Body composition tools for assessment of adult malnutrition at the bedside: A tutorial on research considerations and clinical applications. *Journal of Parenteral and Enteral Nutrition*, 39, 787–822.
- Elmasry, G., & Sun, D. W. (2010). Principles of hyperspectral imaging technology. In *Hyperspectral imaging for food quality & analysis and control* (pp. 3–39). Academic Press Publication.
- EIMasry, G., Wang, N., El Sayed, A., & Ngadi, M. (2007). Hyperspectral imaging for non-destructive determination of some quality attributes for strawberry. *Journal of Food Engineering*, 81(1), 98–107.
- Fernandez, L., Castellero, C., & Aguilera, J. M. (2005). An application of image analysis to dehydration of apple discs. *Journal of Food Engineering*, 67(1–2), 185–193.
- Giavarina, D. (2015). Understanding bland altman analysis. *Biochimica Medica*, 25(2), 141–151.
- Haas, K., Robben, P., Kiesslich, A., Volkert, M., & Jaeger, H. (2019). Stabilization of crystalline carotenoids in carrot concentrate powders: Effects of drying technology, carrier material, and antioxidants. *Food*, 8(8), 285.
- Haeckel, R., Wosniok, W., & Klauke, R. (2013). Comparison of ordinary linear regression, orthogonal regression, standardized principal component analysis, Deming and Passing-Bablok approach for method validation in laboratory medicine: Vergleich von ordinärer linearer regression, orthogonaler regression, standardisierter Hauptkomponentenanalyse, Deming und Passing-Bablok



- Verfahren zur Methodvalidierung in der Laboratoriumsmedizin. *Journal of Laboratory Medicine*, 37(3), 147–163.
- Hanneman, S. K. (2008). Design, analysis and interpretation of method-comparison studies. *AACN Advanced Critical Care*, 19(2), 223–234.
- He, H. J., & Sun, D. W. (2015). Selection of informative spectral wavelength for evaluating and visualising Enterobacteriaceae contamination of salmon flesh. *Food Analytical Methods*, 8(10), 2427–2436.
- Hofman, C. S., Melis, R. J., & Donders, A. R. T. (2015). Adapted Bland-Altman method was used to compare measurement methods with unequal observations per case. *Journal of Clinical Epidemiology*, 68(8), 939–943.
- Horvitz, M. A., Simon, P. W., & Tanumihardjo, S. A. (2004). Lycopene and  $\beta$ -carotene are bioavailable from lycopene 'red'carrots in humans. *European Journal of Clinical Nutrition*, 58(5), 803–811.
- Iglińska-Kalwat, J., Wawrzyńczyk, A., Nowak, I., & Mickiewicz, A. (2012).  $\beta$ -Carotene as an exemplary carotenoid and its application in cosmetic industry. *Chem*, 66(2), 140–144.
- Ihsan, M., Saputro, A. H., & Handayani, W. (2019). Hyperspectral imaging feature selection using regression tree algorithm: Prediction of carotenoid content velvet apple leaf. In *2019 3rd International Conference On Informatics And Computational Sciences (ICICoS)*. (pp. 1–5). IEEE.
- Jun, C.H., Sang-Ho L., Hae-Sang, P. & Jeong-Hwa, L. (2009). Use of partial least squares regression for variable selection and quality prediction. *International Conference on Computers and Industrial Engineering*. 1302–1307. Institute of Electrical and Electronics Engineers. doi: <https://doi.org/10.1109/iccie.2009.5223946>
- Kamal, T., Cheng, S., Khan, I. A., Nawab, K., Zhang, T., Song, Y., Wang, S., Nadeem, M., Riaz, M., Khan, M. A. U., Zhu, B. W., & Tan, M. (2019). Potential uses of LF-NMR and MRI in the study of water dynamics and quality measurement of fruits and vegetables. *Journal of Food Processing and Preservation*, 43(11), e14202.
- Kandpal, L. M., Lee, H., Kim, M. S., Mo, C., & Cho, B. K. (2013). Hyperspectral reflectance imaging technique for visualization of moisture distribution in cooked chicken breast. *Sensors*, 13(10), 13289–13300.
- Khodabakhshian, R., Emadi, B., Khojastehpour, M., Golzarian, M. R., & Sazgarnia, A. (2017). Development of a multispectral imaging system for online quality assessment of pomegranate fruit. *International Journal of Food Properties*, 20(1), 107–118.
- Koca, N., Burdurlu, H. S., & Karadeniz, F. (2007). Kinetics of colour changes in dehydrated carrots. *Journal of Food Engineering*, 78(2), 449–455.
- Larraín, R. E., Schaefer, D. M., & Reed, J. D. (2008). Use of digital images to estimate CIE color coordinates of beef. *Food Research International*, 41(4), 380–385. <https://doi.org/10.1016/j.foodres.2008.01.002>
- Li, X., Li, R., Wang, M., Liu, Y., Zhang, B., & Zhou, J. (2018). Hyperspectral imaging and their applications in the non-destructive quality assessment of fruits and vegetables. In *Hyperspectral imaging in agriculture, food and environment* (pp. 27–63). IntechOpen limited.
- Liu, Y., Sun, Y., Xie, A., Yu, H., Yin, Y., Li, X., & Duan, X. (2017). Potential of hyperspectral imaging for rapid prediction of anthocyanin content of purple-fleshed sweet potato slices during drying process. *Food Analytical Methods*, 10, 3836–3846.
- Liu, C., Liu, W., Lu, X., Chen, W., Yang, J., & Zheng, L. (2016). Potential multispectral imaging for real time determination of colour change and moisture distribution in carrot slices during hot air dehydration. *Food Chemistry*, 195, 110–116.
- Liu, D., Zeng, X. A., & Sun, D. W. (2015). Recent developments and applications of hyperspectral imaging for quality evaluation of agricultural products: A review. *Critical Reviews in Food Science and Nutrition*, 55(12), 1744–1757.
- Lu, Y., Huang, Y., & Lu, R. (2017). Innovative hyperspectral imaging-based techniques for quality evaluation of fruits and vegetables: A review. *Applied Sciences*, 7(2), 189. <https://doi.org/10.3390/app7020189>
- Ludbrook, J. (2010). Linear regression analysis for comparing two measures or methods of measurement: But which regression? *Clinical and Experimental Pharmacology & Physiology*, 37(7), 692–699.
- Md Saleh, R., Kulig, B., Hensel, O., & Sturm, B. (2020). Impact of critical control-point based intermittent drying on drying kinetics and quality of carrot (*Daucus carota* var. laguna). *Thermal Science and Engineering Progress*, 20, 100682. <https://doi.org/10.1016/j.tsep.2020.100682>
- Md Saleh, R., Kulig, B., Hensel, O., & Sturm, B. (2019). Investigation of dynamic quality changes and optimization of drying parameters of carrots (*Daucus carota* var. laguna). *Journal of Food Process Engineering*, 43, e13314. <https://doi.org/10.1111/jfpe.13314>
- Meacham-Hensold, K., Fu, P., Wu, J., Serbin, S., Montes, C. M., Ainsworth, E., Guan, K., Dracup, E., Pederson, T., Driever, S., & Bernacchi, C. (2020). Plot-level rapid screening for photosynthetic parameters using proximal hyperspectral imaging. *Journal of Experimental Botany*, 71(7), 2312–2328.
- Mocák, J., Balla, B., Bobrowski, A., & Blažiček, P. (2003). Proper ways of comparison of two laboratory methods. *Chemical Papers*, 57(3), 143–146.
- Mozaffari, M., Mahmoudi, A., Mollazade, K., & Jamshidi, B. (2016). Low-cost optical approach for noncontact predicting moisture content of apple slices during hot air drying. *Drying Technology*, 35(12), 1530–1542. <https://doi.org/10.1080/07373937.2016.1262394>
- Nguyen, H. H. V., & Nguyen, L. T. (2015). Carrot Processing. In Y. H. Hui & E. Ö. Evranuz (Eds.), *Handbook of Vegetable Preservation and Processing* (pp. 449–466). CRC Press.
- Nicolaï, B. M., Defraeye, T., De Ketelaere, B., Herremans, E., Hertog, M. L., Saeys, W., Torricelli, A., Vandendriessche, T., & Verboven, P. (2014). non-destructive measurement of fruit and vegetable quality. *Annual Review of Food Science and Technology*, 5, 285–312.
- Nicolaï, B.M., Beullens, K., Bobelyn, E., Peirs, A., Saeys, W., Theron, K.I., Lammertyn, & J. Non. (2007) Destructive measurement of fruit and vegetable quality by means of NIR spectroscopy: A review. *Postharvest Biology and Technology*, 46, 99–118.
- Pan, T. T., Sun, D. W., Cheng, J. H., & Pu, H. (2016). Regression algorithms in hyperspectral data analysis for meat quality detection and evaluation. *Comprehensive Reviews in Food Science and Food Safety*, 15(3), 529–541.
- Passing, H., & Bablok, W. (1983). A new biometrical procedure for testing the equality of measurements from two different analytical methods. Application of linear regression procedures for method comparison studies in clinical chemistry. *Part I. Journal of Clinical Chemistry and Clinical Biochemistry*, 21(11), 709–720. <https://doi.org/10.1515/cclm.1983.21.11.709>
- Pu, Y. Y., & Sun, D. W. (2016). Prediction of moisture content uniformity of microwave-vacuum dried mangoes as affected by different shapes using NIR hyperspectral imaging. *Innovative Food Science & Emerging Technologies*, 33, 348–356. <https://doi.org/10.1016/j.ifset.2015.11.003>
- Pu, Y. Y., Yao, Z. F., & Sun, D. W. (2015). Recent progress of hyperspectral imaging on quality and safety inspection of fruits and vegetables: A review. *Comprehensive Reviews in Food Science and Food Safety*, 14, 176–188. <https://doi.org/10.1111/1541-4337.12123>
- Pu, Y. Y., & Sun, D. W. (2015). Vis-NIR hyperspectral imaging in visualizing moisture distribution of mango slices during microwave-vacuum drying. *Food Chemistry*, 188, 271–278.
- Pissard, A., Fernández Pierna, J. A., & Baeten, V. (2013). Non-destructive measurement of vitamin C, total polyphenol and sugar content in apples using near infrared spectroscopy. *Journal of the Science of Food and Agriculture*, 93(2), 238–244.
- Rahman, A., Park, E., Bae, H., & Cho, B. K. (2018). Hyperspectral imaging technique to evaluate the firmness and the sweetness index of tomatoes. *Korean Journal of Agricultural Science*, 45(4), 823–837.

- Rosenfeld, H. J., Samuelsen, R. T., & Lea, P. (1998). The effect of temperature on sensory quality, chemical composition and growth of carrots (*Daucus carota* L.) I. Constant diurnal temperature. *The Journal of Horticultural Science and Biotechnology*, 73(2), 275–288.
- Rungpichayapichet, P., Mahayothee, B., Khuwijtjaru, P., Nagle, M., & Müller, J. (2015). Non-destructive determination of  $\beta$ -carotene content in mango by near infrared spectroscopy compared with colorimetric measurements. *Journal of Food Composition and Analysis*, 38, 32–41.
- Sârbu, C., Liteanu, V., & Bâldea, M. (2000). Evaluation and validation of analytical methods by regression analysis. *Reviews in Analytical Chemistry*, 19, 467–490. <https://doi.org/10.1515/REVAC.2000.19.6.467>
- Schmilovitch, Z., Ignat, T., Alchanatis, V., Gatker, J., Ostrovsky, V., & Felföldi, J. (2014). Hyperspectral imaging of intact bell peppers. *Biosystems Engineering*, 117, 83–93. <https://doi.org/10.1016/j.biosystemseng.2013.07.003>
- Sedgwick, P. (2013). Limits of agreement (Bland-Altman method). *British Medical Journal*, 346, f1630–f1630. <https://doi.org/10.1136/bmj.f1630>
- Sena, M. M., Almeida, M. R., Braga, J. W., & Poppi, R. J. (2017, 2017). Multivariate statistical analysis and chemometrics. In A. S. Franca & L. M. Nollet (Eds.), *Spectroscopic Methods In Food Analysis* (pp. 273–314). CRC Press.
- Shrestha, L., Kulig, B., Moscetti, R., Massantini, R., Pawelzik, E., Hensel, O., & Sturm, B. (2020). Comparison between hyperspectral imaging and chemical analysis of polyphenol oxidase activity on fresh-cut apple slices. *Journal of Spectroscopy*, 2020, 1–10. <https://doi.org/10.1155/2020/7012525>
- Shrestha, L., Crichton, S. O., Kulig, B., Kiesel, B., Hensel, O., & Sturm, B. (2019). Comparative analysis of methods and model prediction performance evaluation for continuous online non-invasive quality assessment during drying of apples from two cultivars. *Thermal Science and Engineering Progress*, 18, 100461. <https://doi.org/10.1016/j.tsep.2019.100461>
- Slavin, J. L., & Lloyd, B. (2012). Health benefits of fruits and vegetables. *Advances in Nutrition*, 3(4), 506–516.
- Sturm, B., Raut, S., Kulig, B., Münsterer, J., Kammhuber, K., Hensel, O., & Crichton, S. O. (2020). In-process investigation of the dynamics in drying behavior and quality development of hops using visual and environmental sensors combined with chemometrics. *Computers and Electronics in Agriculture*, 175, 105547.
- Surbhi, S., Verma, R. C., Deepak, R., Jain, H. K., & Yadav, K. K. (2018). A review: Food, chemical composition and utilization of carrot (*Daucus carota* L.) pomace. *International Journal of Chemical Study*, 6(3), 2921–2926.
- Tian, X. Y., Aheto, J. H., Bai, J. W., Dai, C., Ren, Y., & Chang, X. (2021). Quantitative analysis and visualization of moisture and anthocyanins content in purple sweet potato by Vis-NIR hyperspectral imaging. *Journal of Food Processing and Preservation*, 45(2), e15128.
- Udomkun, P., Nagle, M., Mahayothee, B., & Müller, J. (2014). Laser-based imaging system for non-invasive monitoring of quality changes of papaya during drying. *Food Control*, 42, 225–233.
- van Roy, J., Keresztes, J. C., Wouters, N., De Ketelaere, B., & Saeys, W. (2017). Measuring colour of vine tomatoes using hyperspectral imaging. *Postharvest Biology and Technology*, 129, 79–89.
- von Gersdorff, G. J., Kirchner, S. M., Hensel, O., & Sturm, B. (2021). Impact of drying temperature and salt pre-treatments on drying behavior and instrumental color and investigations on spectral product monitoring during drying of beef slices. *Meat Science*, 178, 108525.
- Wold, S., Sjöström, M., & Eriksson, L. (2001). PLS-regression: A basic tool of chemometrics. *Chemometrics and Intelligent Laboratory Systems*, 58(2), 109–130.
- Wu, D., & Sun, D. W. (2013). Hyperspectral imaging technology: A non-destructive tool for food quality and safety evaluation and inspection. In *Advances in food Process Engineering Research and Applications* (pp. 581–606). Springer.
- Yu, P., Huang, M., Zhang, M., Zhu, Q., & Qin, J. (2020). Rapid detection of moisture content and shrinkage ratio of dried carrot slices by using a multispectral imaging system. *Infrared Physics & Technology*, 108, 103361.
- Yu, P., Huang, M., Zhang, M., & Yang, B. (2019). Optimal wavelength selection for hyperspectral imaging evaluation on vegetable soybean moisture content during drying. *Applied Sciences*, 9(2), 331.
- Zhang, L., Sun, J., Zhou, X., Nirere, A., Wu, X., & Dai, R. (2020). Classification detection of saccharin jujube based on hyperspectral imaging technology. *Journal of Food Processing and Preservation*, 44(8), e14591.
- Zhang, B., Dai, D., Huang, J., Zhou, J., Gui, Q., & Dai, F. (2018). Influence of physical and biological variability and solution methods in fruit and vegetable quality non-destructive inspection by using imaging and near-infrared spectroscopy techniques: A review. *Critical Reviews in Food Science and Nutrition*, 58(12), 2099–2118.
- Zhang, B., Gu, B., Tian, G., Zhou, J., Huang, J., & Xiong, Y. (2018). Challenges and solutions of optical-based non-destructive quality inspection for robotic fruit and vegetable grading systems: A technical review. *Trends in Food Science & Technology*, 81, 213–231. <https://doi.org/10.1016/j.tifs.2018.09.018>
- Zhang, B., Li, J., Fan, S., Huang, W., Zhao, C., Liu, C., & Huang, D. (2015). Hyperspectral imaging combined with multivariate analysis and band math for detection of common defects on peaches (*Prunus persica*). *Computers and Electronics in Agriculture*, 114, 14–24.
- Zhao, D., An, K., Ding, S., Liu, L., Xu, Z., & Wang, Z. (2014). Two-stage intermittent microwave coupled with hot-air drying of carrot slices: Drying kinetics and physical quality. *Food and Bioprocess Technology*, 7(8), 2308–2318.
- Zude, M., Spinelli, L., & Torricelli, A. (2008). Approach for non-destructive pigment analysis in model liquids and carrots by means of time-of-flight and multi-wavelength remittance readings. *Analytica Chimica Acta*, 623(2), 204–212. <https://doi.org/10.1016/j.aca.2008.06.014>
- Zude, M., Birlouez-Aragon, I., Paschold, P.-J., & Rutledge, D. N. (2007). Non-invasive spectrophotometric sensing of carrot quality from harvest to consumption. *Postharvest Biology and Technology*, 45(1), 30–37. <https://doi.org/10.1016/j.postharvbio.2007.01.010>

**How to cite this article:** Md Saleh, R., Kulig, B., Arefi, A., Hensel, O. & Sturm, B. (2022). Prediction of total carotenoids, color, and moisture content of carrot slices during hot air drying using non-invasive hyperspectral imaging technique. *Journal of Food Processing and Preservation*, 46, e16460. <https://doi.org/10.1111/jfpp.16460>